Oblique Rayleigh wave scattering by a cylindrical cavity

C M Linton, Department of Mathematical Sciences,
Loughborough University, Leicestershire, LE11 3TU, UK
I Thompson, Department of Mathematical Sciences,
University of Liverpool, Liverpool L69 7ZL, UK

Abstract

The problem of oblique wave scattering of a Rayleigh wave by a cylindrical cavity in an elastic half-space is solved using the multipole expansion method. Whereas in the analogous water-wave problem a single scalar field is expressed as an infinite multipole expansion, and in the Rayleigh wave case with normal incidence two scalar fields suffice, here we require three coupled scalar multipole expansions. The focus of our numerical results is on the energy scattered by the cavity and in particular the proportion of the incident wave energy that is reflected and transmitted in the form of Rayleigh waves and the proportion that is transformed into cylindrical bulk waves which propagate into the half-space.

1 Introduction

The problem considered in this paper is that of the interaction between a Rayleigh wave on an elastic half-space and a horizontal circular cylindrical cavity, the generators of the cylinder making an arbitrary angle with the direction of propagation of the Rayleigh wave. The particular focus is on the far field that results and a computation of how the energy in the scattered field is distributed between reflected and transmitted Rayleigh waves and the cylindrical P- and S-waves that are generated.

There is a natural analogue to this problem in the linear theory of water waves (scattering by a submerged rigid cylinder) and in that context Ursell [1, 2] introduced a solution technique for the case of normal incidence based on multipole expansions. The multipoles are solutions to the governing equation (Laplace's equation) which are singular at the centre of the cylinder and which satisfy the appropriate free-surface boundary condition. The scattered field is expressed as a linear combination of these multipoles and application of the boundary condition on the surface of the cylinder leads to an infinite linear system of algebraic equations which, with modern computational tools, can easily be solved by truncation to an $N \times N$ system with N sufficiently large. The extension of this technique to obliquely incident waves was developed in [3].

Gregory [4] recognised that multipole expansions could be used for scattering problems involving cavities in a half-space and an application of the theory to problems where the scatterer is a cylindrical cavity appears in [5]. Only the two-dimensional problem which results when the incident wave is normal to the cylindrical cavity was considered and there are two additional complications which arise when compared with the water wave problem. The first is that the field is described by a pair of coupled scalar potentials rather than a single one and the second is that the far field contains both surface waves and cylindrical bulk waves. Nevertheless, Gregory was able to prove some theorems about the validity of the expansions used, calculate the asymptotic form of the multipoles which are needed to determine the far field, and derive some results applicable in the long-wave limit.

The problem studied by Gregory has been revisited on many occasions, usually with some approximation or simplification to make it more tractable. For example, if instead of a Rayleigh wave the incident field is taken as a bulk SH-wave then the problem can be solved simply using the method of images and this idea was used in [6] to analyse the diffraction of SH-waves by a cavity with an elastic lining. An extension to inclusions of arbitrary shape can be found in [7], and [8] is a more detailed study, allowing for both plane and cylindrical incident waves on a circular inclusion.

One of the key difficulties in the problem is the juxtaposition of a cylindrical and a plane boundary. One approach to removing this problem is to approximate the free surface, when necessary, as a cylindrical surface with large radius. This allows for more straightforward algebraic calculations, but it is not at all clear when the solutions are likely to correspond accurately to those of the actual problem under consideration. Examples of this approach can be found in [9] and [10]. Another solution procedure was introduced in [11]. The scattered field is expressed in terms of Gregory's multipole expansions but instead of applying the boundary condition on the cylinder surface exactly, an approach based on matched asymptotic expansions is applied — equivalent to a long-wave (i.e. low-frequency) approximation. This technique was extended to the case of scattering by cylindrical shells in [12, 13].

In [11], Gregory's method is described as "rather cumbersome" and in [9] it is noted that Gregory's solution "contains complicated contour integrals which are difficult to evaluate numerically". The latter statement is certainly no longer true, though care does need to be taken, and while it is true that some lengthy calculations are required, Gregory's method seems no more cumbersome than any of the other techniques available. In this paper we have extended Gregory's approach to the case of oblique incidence. This introduces some additional complications, most notably that the field must now be expressed in terms of three coupled potentials. Also, the nature of the far field changes depending on the angle of incidence. For normal and small angles of incidence the scattered field is made up of reflected and transmitted Rayleigh waves together with cylindrical P- and S-waves. Above some critical angle the P-wave disappears and then above a second critical angle, the S-wave is not present either. Our key objective is to illustrate this phenomenon by showing how the scattered energy is distributed between these different waves as the angle of incidence or the frequency varies. It is possible to derive relations which express conservation of energy for our problem and in order to do this we have extended results of [14] which were derived for normal incidence in a manner analogous to Newman's work on water waves [15]. An alternative approach to the derivation of these relations, again for normal incidence, is given in [16].

Previous work on the oblique incidence problem appears rather limited. In [17] an integral equation formulation was used to study the motion of the ground near a cavity and the stresses on the cavity wall and in [18] oblique incidence on a submerged, lined, cavity using a T-matrix formalism was considered. In neither case was any attempt made to study the far field.

In the water wave context, it has been known for a long time that a submerged circular cylinder can support trapped modes. These are waves that propagate parallel to the cylinder axis and decay exponentially away from the cylinder. Their existence was established by Ursell [19] and numerical computations of the dispersion curves for these waves can be found in [20]. It is highly likely that similar modes exist for a cylindrical cavity in a half-space. We intend to investigate these trapped modes in a subsequent paper. Modes will be sought with wavenumbers which are greater than that for which Rayleigh waves exist, i.e. in a regime

where it is not possible to formulate a scattering problem of the type considered in this paper ($\ell > k_{\rm R}$; see §3 below). In contrast to the water wave problem, the situation is complicated by the fact that a cylindrical cavity in an otherwise unbounded medium supports modes which travel along its surface, parallel to the cylinder axis [21], [22]. These modes exist for values of ℓ in the range $k_2 < \ell < k_{\rm R}$ which is covered by the analysis in this paper. The presence of Rayleigh waves means that these modes do not exist in our problem because the energy associated with them would leak away from the cavity along the free surface. However, as we will note in §5 they do influence our results in a qualitative way.

In §2 we formulate the boundary value problem corresponding to scattering by a cavity in a half-space. We use the Helmholtz decomposition for the displacement field and hence represent the solution in terms of three scalar fields each of which satisfies a Helmholtz equation, and the stress free boundary conditions on the free surface and on the cavity wall are expressed in terms of these three functions. In §3 the scattering problem in which the incident wave is a Rayleigh wave is described and the boundary conditions applied to yield an infinite system of linear algebraic equations. Our focus in this paper is on the scattered energy and we describe the form of the far field, including the energy balance for this problem, in §4. Finally, we present numerical results in §5. Many technical details are relegated to appendices.

2 Formulation

The region $z < 0$ is a homogeneous and isotropic elastic medium containing a cylindrical cavity aligned with the y-axis. Unit vectors in the x-, y- and z-directions are denoted by $\mathbf{e}_x$, $\mathbf{e}_y$ and $\mathbf{e}_z$, respectively. The boundary $z = 0$ is stress free. We wish to investigate the scattering of an obliquely incident Rayleigh wave by the cavity. We introduce polar coordinates centred at the point $x = 0$, $z = -h$ via $r\sin\theta = x$, $r\cos\theta = -(z+h)$. Thus θ is measured from the downward vertical and the cavity is the region $r < a$.

We consider time-harmonic motion with frequency $\omega > 0$, suppress an $\exp(-{\rm i}\omega t)$ dependence, and then the displacement field satisfies Navier's equation

$$c_1^2\nabla(\nabla\cdot\mathbf{u}) - c_2^2\nabla\times(\nabla\times\mathbf{u}) = -\omega^2\mathbf{u}. \tag{2.1}$$

Here

$$c_1^2 = (\lambda+2\mu)/\rho, \qquad c_2^2 = \mu/\rho, \tag{2.2}$$

in which λ and μ are the Lamé constants related to the Young's modulus E and Poisson's ratio σ via

$$\lambda = \frac{E\sigma}{(1-2\sigma)(1+\sigma)}, \qquad \mu = \frac{E}{2(1+\sigma)} \tag{2.3}$$

and ρ is the density of the elastic medium. For most materials $0 < \sigma < 1/2$, but $-1 < \sigma \leq 0$ is also possible. Note that $\lambda+\mu = E/[2(1+\sigma)(1-2\sigma)] > 0$ and so we always have $c_1^2 > c_2^2$. The quantity c_1 is the wave speed for longitudinal (pressure, primary or P-) waves in an infinite medium, whereas c_2 is the speed of transverse (shear, secondary or S-) waves. We introduce corresponding wavenumbers $k_i = \omega/c_i$. The ratio

$$\Lambda = \frac{k_1^2}{k_2^2} = \frac{c_2^2}{c_1^2} = \frac{1-2\sigma}{2(1-\sigma)} \tag{2.4}$$

does not depend on E and we have $0 < \Lambda < 3/4$. Note that $\rho\omega^2 = \mu k_2^2$ and $\lambda + 2\mu = \mu/\Lambda$.

We utilise the Helmholtz decomposition of the displacement field

$$\mathbf{u} = \nabla\Phi + \nabla \times \mathbf{\Psi}, \qquad \nabla \cdot \mathbf{\Psi} = 0, \tag{2.5}$$

with

$$\Phi = \phi(x,z)\mathrm{e}^{\mathrm{i}\ell y}, \quad \mathbf{\Psi} = \psi(x,z)\mathrm{e}^{\mathrm{i}\ell y}\mathbf{e}_y + \frac{\mathrm{i}\ell}{k_2^2}\nabla\left(\psi(x,z)\mathrm{e}^{\mathrm{i}\ell y}\right) + \frac{1}{k_2}\nabla \times \left(\chi(x,z)\mathrm{e}^{\mathrm{i}\ell y}\mathbf{e}_y\right) \tag{2.6}$$

and then ϕ, ψ and χ satisfy the two-dimensional scalar Helmholtz equations

$$(\nabla_{xz}^2 + \kappa_1^2)\phi = 0, \qquad (\nabla_{xz}^2 + \kappa_2^2)\psi = (\nabla_{xz}^2 + \kappa_2^2)\chi = 0. \tag{2.7}$$

For convenience we have defined

$$\kappa_i^2 = k_i^2 - \ell^2 \tag{2.8}$$

and $\nabla_{xz}^2 \equiv \partial_x^2 + \partial_z^2$. If $\kappa_i^2 > 0$ we take $\kappa_i > 0$, whereas if $\kappa_i^2 < 0$ we take $\kappa_i = \mathrm{i}q_i$, $q_i > 0$. In this formulation, ϕ represents the irrotational component of the field while ψ and χ together represent the divergence-free component. We have $\mathbf{u} = \mathrm{e}^{\mathrm{i}\ell y}\tilde{\mathbf{u}}$, where

$$\tilde{\mathbf{u}} = \nabla_{xz}\phi + \mathrm{i}\ell\phi\,\mathbf{e}_y + \nabla_{xz}\psi \times \mathbf{e}_y + \frac{\kappa_2^2}{k_2}\chi\mathbf{e}_y + \frac{\mathrm{i}\ell}{k_2}\nabla_{xz}\chi \tag{2.9}$$

$$= \left(\phi_x - \psi_z + \frac{\mathrm{i}\ell}{k_2}\chi_x\right)\mathbf{e}_x + \left(\mathrm{i}\ell\phi + \frac{\kappa_2^2}{k_2}\chi\right)\mathbf{e}_y + \left(\phi_z + \psi_x + \frac{\mathrm{i}\ell}{k_2}\chi_z\right)\mathbf{e}_z \tag{2.10}$$

and

$$\nabla \cdot \mathbf{u} = -k_1^2\phi\,\mathrm{e}^{\mathrm{i}\ell y}. \tag{2.11}$$

The components of the stress tensor are given by

$$\tau_{11} = \mathrm{e}^{\mathrm{i}\ell y}\left(-\lambda k_1^2\phi + 2\mu\left(\phi_{xx} - \psi_{xz} + \frac{\mathrm{i}\ell}{k_2}\chi_{xx}\right)\right), \tag{2.12}$$

$$\tau_{12} = \tau_{21} = \mu\mathrm{e}^{\mathrm{i}\ell y}\left(2\mathrm{i}\ell\phi_x - \mathrm{i}\ell\psi_z + \frac{\nu^2}{k_2}\chi_x\right), \tag{2.13}$$

$$\tau_{13} = \tau_{31} = \mu\mathrm{e}^{\mathrm{i}\ell y}\left(2\phi_{xz} + \psi_{xx} - \psi_{zz} + \frac{2\mathrm{i}\ell}{k_2}\chi_{xz}\right), \tag{2.14}$$

$$\tau_{23} = \tau_{32} = \mu\mathrm{e}^{\mathrm{i}\ell y}\left(2\mathrm{i}\ell\phi_z + \mathrm{i}\ell\psi_x + \frac{\nu^2}{k_2}\chi_z\right), \tag{2.15}$$

$$\tau_{33} = \mathrm{e}^{\mathrm{i}\ell y}\left(-\lambda k_1^2\phi + 2\mu\left(\phi_{zz} + \psi_{xz} + \frac{\mathrm{i}\ell}{k_2}\chi_{zz}\right)\right), \tag{2.16}$$

where we have written

$$\nu^2 = \kappa_2^2 - \ell^2 = k_2^2 - 2\ell^2. \tag{2.17}$$

On $z = 0$ we require zero traction which in turn means that the components τ_{13}, τ_{23} and τ_{33} of the stress tensor must vanish there. Hence

$$2\phi_{xz} + \psi_{xx} - \psi_{zz} + \frac{2\mathrm{i}\ell}{k_2}\chi_{xz} = 0 \qquad \text{on } z = 0, \tag{2.18}$$

$$2\mathrm{i}\ell\phi_z + \mathrm{i}\ell\psi_x + \frac{\nu^2}{k_2}\chi_z = 0 \qquad \text{on } z = 0, \tag{2.19}$$

$$-\lambda k_1^2\phi + 2\mu\left(\phi_{zz} + \psi_{xz} + \frac{\mathrm{i}\ell}{k_2}\chi_{zz}\right) = 0 \qquad \text{on } z = 0. \tag{2.20}$$

An alternative form for (2.18) is

$$2(\phi_{xz}+\psi_{xx})+\kappa_2^2\psi+\frac{2\mathrm{i}\ell}{k_2}\chi_{xz}=0 \qquad \text{on } z=0, \tag{2.21}$$

whilst an alternative form for (2.20) is

$$2(\psi_{xz}-\phi_{xx})-\nu^2\phi+\frac{2\mathrm{i}\ell}{k_2}\chi_{zz}=0 \qquad \text{on } z=0. \tag{2.22}$$

In terms of cylindrical coordinates (r,θ,y) with associated unit vectors $\mathbf{e}_r$, $\mathbf{e}_\theta$ and $\mathbf{e}_y$ we have

$$\mathbf{e}_r=\sin\theta\,\mathbf{e}_x-\cos\theta\,\mathbf{e}_z, \quad \mathbf{e}_\theta=\cos\theta\,\mathbf{e}_x+\sin\theta\,\mathbf{e}_z \tag{2.23}$$

and we note that with the order θ, r, y the system is right-handed. From (2.10) we obtain

$$\tilde{\mathbf{u}}=\left(\phi_r-\frac{1}{r}\psi_\theta+\frac{\mathrm{i}\ell}{k_2}\chi_r\right)\mathbf{e}_r+\left(\frac{1}{r}\phi_\theta+\psi_r+\frac{\mathrm{i}\ell}{k_2 r}\chi_\theta\right)\mathbf{e}_\theta+\left(\mathrm{i}\ell\phi+\frac{\kappa_2^2}{k_2}\chi\right)\mathbf{e}_y. \tag{2.24}$$

If we want to impose the condition of zero traction on the surface $r=a$ then, since the normal is in the direction of $\mathbf{e}_r$, we require the three components τ_{rr}, $\tau_{\theta r}$ and τ_{yr} to vanish. Now

$$\tau_{rr}=-k_1^2\lambda\phi\,\mathrm{e}^{\mathrm{i}\ell y}+2\mu e_{rr}, \quad \tau_{\theta r}=2\mu e_{\theta r}, \quad \tau_{yr}=2\mu e_{yr}, \tag{2.25}$$

where the components of the strain tensor are given by [23, p. 304]

$$e_{rr}=u_{r,r}=\mathrm{e}^{\mathrm{i}\ell y}\left(\phi_{rr}+\frac{1}{r^2}\psi_\theta-\frac{1}{r}\psi_{r\theta}+\frac{\mathrm{i}\ell}{k_2}\chi_{rr}\right), \tag{2.26}$$

$$e_{yr}=\frac{\mathrm{e}^{\mathrm{i}\ell y}}{2}\left(2\mathrm{i}\ell\phi_r-\frac{\mathrm{i}\ell}{r}\psi_\theta+\frac{\nu^2}{k_2}\chi_r\right), \tag{2.27}$$

$$e_{\theta r}=\frac{\mathrm{e}^{\mathrm{i}\ell y}}{2}\left(\frac{2}{r}\phi_{r\theta}-\frac{1}{r^2}\psi_{\theta\theta}+\frac{2\mathrm{i}\ell}{k_2 r}\chi_{r\theta}+\psi_{rr}-\frac{2}{r^2}\phi_\theta-\frac{1}{r}\psi_r-\frac{2\mathrm{i}\ell}{k_2 r^2}\chi_\theta\right). \tag{2.28}$$

We thus have the boundary conditions

$$-k_1^2\lambda\phi+2\mu\left(\phi_{rr}+\frac{1}{a^2}\psi_\theta-\frac{1}{a}\psi_{r\theta}+\frac{\mathrm{i}\ell}{k_2}\chi_{rr}\right)=0, \qquad \text{on } r=a, \tag{2.29}$$

$$2\mathrm{i}\ell\phi_r-\frac{\mathrm{i}\ell}{a}\psi_\theta+\frac{\nu^2}{k_2}\chi_r=0, \qquad \text{on } r=a, \tag{2.30}$$

$$\frac{2}{a}\phi_{r\theta}-\frac{2}{a^2}\phi_\theta-\frac{1}{a^2}\psi_{\theta\theta}+\psi_{rr}-\frac{1}{a}\psi_r+\frac{2\mathrm{i}\ell}{k_2 a}\chi_{r\theta}-\frac{2\mathrm{i}\ell}{k_2 a^2}\chi_\theta=0, \qquad \text{on } r=a. \tag{2.31}$$

3 Scattering problem

We will consider the incident field to be a Rayleigh wave propagating at an angle θ_{inc} to the x-axis ($0\le\theta_{\mathrm{inc}}<\pi/2$). Thus we take $\ell=k_{\mathrm{R}}\sin\theta_{\mathrm{inc}}\ge 0$, $\alpha=k_{\mathrm{R}}\cos\theta_{\mathrm{inc}}>0$, introduce the vectors

$$\mathbf{c}_\pm=\pm\mathrm{i}\alpha\,\mathbf{e}_x+\mathrm{i}\ell\,\mathbf{e}_y+\beta_1\mathbf{e}_z, \quad \mathbf{d}_\pm=\mp\frac{\beta_2\alpha}{k_{\mathrm{R}}}\mathbf{e}_x-\frac{\beta_2\ell}{k_{\mathrm{R}}}\mathbf{e}_y+\mathrm{i}k_{\mathrm{R}}\mathbf{e}_z \tag{3.1}$$

and then

$$\tilde{\mathbf{u}}_{\rm inc} = C\mathrm{e}^{\mathrm{i}\alpha x}\mathrm{e}^{\beta_1 z}\mathbf{c}_+ + D\mathrm{e}^{\mathrm{i}\alpha x}\mathrm{e}^{\beta_2 z}\mathbf{d}_+, \tag{3.2}$$

where

$$\beta_i = \left(k_{\rm R}^2 - k_i^2\right)^{1/2} \tag{3.3}$$

and we have

$$0 \le \ell < k_{\rm R}, \qquad 0 < k_1 < k_2 < k_{\rm R}, \qquad 0 < \beta_2 < \beta_1 < k_{\rm R}. \tag{3.4}$$

Here $k_{\rm R}$ is the unique real root of

$$4k_{\rm R}^2\beta_1\beta_2 = (k_{\rm R}^2 + \beta_2^2)^2 \tag{3.5}$$

for which $0 < k_2/k_{\rm R} < 1$ and C/D is determined from the equation

$$\frac{C}{D} = -\frac{2\mathrm{i}\beta_2 k_{\rm R}}{k_{\rm R}^2 + \beta_2^2} = \frac{k_{\rm R}^2 + \beta_2^2}{2\mathrm{i}\beta_1 k_{\rm R}}. \tag{3.6}$$

Note that

$$|C|^2/|D|^2 = \beta_2/\beta_1. \tag{3.7}$$

This incident field can be described by the triple $\{\phi_{\rm inc}, \psi_{\rm inc}, \chi_{\rm inc}\}$, where

$$\phi_{\rm inc} = C\mathrm{e}^{\mathrm{i}\alpha x}\mathrm{e}^{\beta_1 z}, \quad \psi_{\rm inc} = D_\psi\mathrm{e}^{\mathrm{i}\alpha x}\mathrm{e}^{\beta_2 z}, \quad \chi_{\rm inc} = D_\chi\mathrm{e}^{\mathrm{i}\alpha x}\mathrm{e}^{\beta_2 z}, \tag{3.8}$$

$$D_\psi = \frac{Dk_2^2\alpha}{\kappa_2^2 k_{\rm R}}, \quad D_\chi = -\frac{D\beta_2 k_2 \ell}{\kappa_2^2 k_{\rm R}}. \tag{3.9}$$

When $\ell = 0$ (normal incidence), $D_\psi = D$ and $D_\chi = 0$. Note that although $\psi_{\rm inc}$ and $\chi_{\rm inc}$ are singular when $\ell = k_2$ ($\kappa_2 = 0$), the combinations $\psi_z - (\mathrm{i}\ell/k_2)\chi_x$ and $\psi_x + (\mathrm{i}\ell/k_2)\chi_z$, which occur in (2.10), are not. These functions can be expanded about $r = 0$ in the form

$$\begin{gathered}\phi_{\rm inc} = \sum_{n=-\infty}^{\infty} A_n^{\rm inc}\,\mathrm{J}_n(\kappa_1 r)\mathrm{e}^{\mathrm{i}n\theta}, \quad \psi_{\rm inc} = \sum_{n=-\infty}^{\infty} B_n^{\rm inc}\,\mathrm{J}_n(\kappa_2 r)\mathrm{e}^{\mathrm{i}n\theta}, \\ \chi_{\rm inc} = \sum_{n=-\infty}^{\infty} C_n^{\rm inc}\,\mathrm{J}_n(\kappa_2 r)\mathrm{e}^{\mathrm{i}n\theta}.\end{gathered} \tag{3.10}$$

To accomplish this we define ζ_i according to $\alpha = \kappa_i\cosh\zeta_i$, $\beta_i = \kappa_i\sinh\zeta_i$, i.e.,

$$\mathrm{e}^{\zeta_i} = (\alpha + \beta_i)/\kappa_i, \qquad \mathrm{e}^{-\zeta_i} = (\alpha - \beta_i)/\kappa_i. \tag{3.11}$$

In other words, if $\kappa_i = \mathrm{i}q_i$, $q_i > 0$, then

$$\zeta_i = -\frac{\pi\mathrm{i}}{2} + \sinh^{-1}\frac{\alpha}{q_i}. \tag{3.12}$$

On the other hand, if $\kappa_i > 0$ is real we have $0 < \kappa_i < \alpha$ and

$$\zeta_i = \cosh^{-1}\frac{\alpha}{\kappa_i}. \tag{3.13}$$

Then

$$\mathrm{e}^{\beta_i z}\mathrm{e}^{\mathrm{i}\alpha x} = \mathrm{e}^{-\beta_i h}\mathrm{e}^{\mathrm{i}\kappa_i r\sin(\mathrm{i}\zeta_i+\theta)} = \mathrm{e}^{-\beta_i h}\sum_{n=-\infty}^{\infty}\mathrm{J}_n(\kappa_i r)\mathrm{e}^{\mathrm{i}n\theta}\mathrm{e}^{-n\zeta_i}, \tag{3.14}$$

using Jacobi's expansion [24, §2.22], and so

$$A_n^{\rm inc} = C\mathrm{e}^{-\beta_1 h}\mathrm{e}^{-n\zeta_1}, \quad B_n^{\rm inc} = D_\psi \mathrm{e}^{-\beta_2 h}\mathrm{e}^{-n\zeta_2}, \quad C_n^{\rm inc} = D_\chi \mathrm{e}^{-\beta_2 h}\mathrm{e}^{-n\zeta_2}. \tag{3.15}$$

Although these coefficients can grow (exponentially) as $|n|$ increases, the expansions (3.10) converge, since, for $x \in \mathbb{R}$, both $\mathrm{J}_n(x)$ and $\mathrm{I}_n(x) = \mathrm{i}^{-n}\,\mathrm{J}_n(\mathrm{i}x)$ behave like $(2\pi n)^{-1/2}(\mathrm{e}x/2n)^n$ as $n \to \infty$.

We now expand the scattered field in terms of multipoles by writing

$$\tilde{\mathbf{u}} = \tilde{\mathbf{u}}_{\rm inc} + \tilde{\mathbf{u}}_{\rm sc} = \tilde{\mathbf{u}}_{\rm inc} + \sum_{n,i} \xi_n^{(i)} \tilde{\mathbf{u}}_n^{(i)}, \tag{3.16}$$

where $\xi_n^{(i)}$ are unknowns to be determined, $\tilde{\mathbf{u}}_n^{(i)}$ are multipoles defined in Appendix A, and $\sum_{n,i}$ is shorthand for $\sum_{n=-\infty}^{\infty}\sum_{i=1}^{3}$. Thus if $\tilde{\mathbf{u}}$ is given by the triple $\{\phi, \psi, \chi\}$ we have

$$\phi = \phi_{\rm inc} + \sum_{n,i} \xi_n^{(i)} \phi_n^{(i)} \tag{3.17}$$

$$= \sum_{m=-\infty}^{\infty} \mathrm{e}^{\mathrm{i}m\theta} \left(A_m^{\rm inc}\,\mathrm{J}_m(\kappa_1 r) + \xi_m^{(1)}\,\mathrm{H}_m(\kappa_1 r) + \sum_{n,i} \xi_n^{(i)} A_{nm}^{(i)}\,\mathrm{J}_m(\kappa_1 r) \right). \tag{3.18}$$

Similarly

$$\psi = \sum_{m=-\infty}^{\infty} \mathrm{e}^{\mathrm{i}m\theta} \left(B_m^{\rm inc}\,\mathrm{J}_m(\kappa_2 r) + \xi_m^{(2)}\,\mathrm{H}_m(\kappa_2 r) + \sum_{n,i} \xi_n^{(i)} B_{nm}^{(i)}\,\mathrm{J}_m(\kappa_2 r) \right), \tag{3.19}$$

$$\chi = \sum_{m=-\infty}^{\infty} \mathrm{e}^{\mathrm{i}m\theta} \left(C_m^{\rm inc}\,\mathrm{J}_m(\kappa_2 r) + \xi_m^{(3)}\,\mathrm{H}_m(\kappa_2 r) + \sum_{n,i} \xi_n^{(i)} C_{nm}^{(i)}\,\mathrm{J}_m(\kappa_2 r) \right). \tag{3.20}$$

It is convenient to introduce the notation

$$J_{ni} = \mathrm{J}_n(\overline{\kappa}_i), \quad J'_{ni} = \overline{\kappa}_i\,\mathrm{J}'_n(\overline{\kappa}_i), \quad J''_{ni} = \overline{\kappa}_i^2\,\mathrm{J}''_n(\overline{\kappa}_i), \tag{3.21}$$

$$H_{ni} = \mathrm{H}_n(\overline{\kappa}_i), \quad H'_{ni} = \overline{\kappa}_i\,\mathrm{H}'_n(\overline{\kappa}_i), \quad H''_{ni} = \overline{\kappa}_i^2\,\mathrm{H}''_n(\overline{\kappa}_i), \tag{3.22}$$

where an overbar indicates that a quantity has been non-dimenionalised with respect to a, and we note that

$$J''_{ni} + J'_{ni} + \left(\overline{\kappa}_i^2 - n^2\right) J_{ni} = 0, \tag{3.23}$$

with the equivalent equation for the H_{ni} terms. We also write

$$\mathcal{J}_{ni} = J'_{ni} - J_{ni}, \quad \widetilde{\mathcal{J}}_{n1} = (2n^2 - \overline{\nu}^2)J_{n1} - 2J'_{n1}, \quad \widetilde{\mathcal{J}}_{n2} = (2n^2 - \overline{\kappa}_2^2)J_{n2} - 2J'_{n2} \tag{3.24}$$

with equivalent expressions formed by replacing $\mathcal{J}$ and J with $\mathcal{H}$ and H, respectively. We also have

$$\mu\widetilde{\mathcal{J}}_{m1} = -\overline{k}_1^2\lambda J_{m1} + 2\mu J''_{m1} \tag{3.25}$$

which relies on the fact that $k_1^2\lambda + 2\mu\kappa_1^2 = \mu\nu^2$.

The boundary condition (2.29) then yields

$$\widetilde{\mathcal{H}}_{m1}\xi_m^{(1)} - 2\mathrm{i}m\mathcal{H}_{m2}\xi_m^{(2)} + \frac{2\mathrm{i}\ell}{k_2}H''_{m2}\xi_m^{(3)} + \sum_{n,i}\xi_n^{(i)}\left[\widetilde{\mathcal{J}}_{m1}A_{nm}^{(i)} - 2\mathrm{i}m\mathcal{J}_{m2}B_{nm}^{(i)} + \frac{2\mathrm{i}\ell}{k_2}J''_{m2}C_{nm}^{(i)}\right]$$

$$= -\widetilde{\mathcal{J}}_{m1}A_m^{\rm inc} + 2\mathrm{i}m\mathcal{J}_{m2}B_m^{\rm inc} - \frac{2\mathrm{i}\ell}{k_2}J''_{m2}C_m^{\rm inc}, \tag{3.26}$$

to be satisfied for each $m \in \mathbb{Z}$ due to orthogonality. Similarly, the boundary condition (2.30) yields

$$2\mathrm{i}\overline{\ell}H'_{m1}\xi^{(1)}_m + m\overline{\ell}H_{m2}\xi^{(2)}_m + \frac{\overline{\nu}^2}{\overline{k}_2}H'_{m2}\xi^{(3)}_m + \sum_{n,i}\xi^{(i)}_n\left[2\mathrm{i}\overline{\ell}J'_{m1}A^{(i)}_{nm} + m\overline{\ell}J_{m2}B^{(i)}_{nm} + \frac{\overline{\nu}^2}{\overline{k}_2}J'_{m2}C^{(i)}_{nm}\right]$$
$$= -2\mathrm{i}\overline{\ell}J'_{m1}A^{\mathrm{inc}}_m - m\overline{\ell}J_{m2}B^{\mathrm{inc}}_m - \frac{\overline{\nu}^2}{\overline{k}_2}J'_{m2}C^{\mathrm{inc}}_m, \quad (3.27)$$

and the boundary condition (2.31) yields

$$2\mathrm{i}m\mathcal{H}_{m1}\xi^{(1)}_m + \widetilde{\mathcal{H}}_{m2}\xi^{(2)}_m - \frac{2m\ell}{k_2}\mathcal{H}_{m2}\xi^{(3)}_m + \sum_{n,i}\xi^{(i)}_n\left[2\mathrm{i}m\mathcal{J}_{m1}A^{(i)}_{nm} + \widetilde{\mathcal{J}}_{m2}B^{(i)}_{nm} - \frac{2m\ell}{k_2}\mathcal{J}_{m2}C^{(i)}_{nm}\right]$$
$$= -2\mathrm{i}m\mathcal{J}_{m1}A^{\mathrm{inc}}_m - \widetilde{\mathcal{J}}_{m2}B^{\mathrm{inc}}_m + \frac{2m\ell}{k_2}\mathcal{J}_{m2}C^{\mathrm{inc}}_m, \quad (3.28)$$

to be satisfied for each $m \in \mathbb{Z}$ in each case, where we have used (3.23) to replace J''_{m2} and H''_{m2}. The unknown coefficients $A^{(i)}_{nm}$, $B^{(i)}_{nm}$ and $C^{(i)}_{nm}$ can then be determined by converting (3.26), (3.27) and (3.28) into a single infinite system of equations and then solving by truncation.

This system can be reduced to a pair of smaller systems by separating its symmetric and antisymmetric components. From (2.10), we observe that if ϕ and χ are symmetric across $x = 0$ and ψ is antisymmetric, then u is symmetric, and vice-versa. We then define

$$\phi^{\mathrm{s}}_{\mathrm{inc}} = \frac{C}{2}\,\mathrm{e}^{\beta_1 z}(\mathrm{e}^{\mathrm{i}\alpha x} + \mathrm{e}^{-\mathrm{i}\alpha x}) \quad \text{and} \quad \phi^{\mathrm{a}}_{\mathrm{inc}} = \frac{C}{2}\,\mathrm{e}^{\beta_1 z}(\mathrm{e}^{\mathrm{i}\alpha x} - \mathrm{e}^{-\mathrm{i}\alpha x}), \quad (3.29)$$

and likewise for χ and ψ. For the case where the irrotational component of the field is symmetric, we must have

$$A^{\mathrm{inc}}_{-n} = (-1)^n A^{\mathrm{inc}}_n, \quad B^{\mathrm{inc}}_{-n} = (-1)^{n+1}B^{\mathrm{inc}}_n \quad \text{and} \quad C^{\mathrm{inc}}_{-n} = (-1)^n C^{\mathrm{inc}}_n \quad (3.30)$$

in (3.10). Changing θ to $-\theta$ and m to $-m$ in (3.18–3.20) and using (A.31) shows that the scattered field has the same symmetries if

$$\xi^{(i)}_{-n} = (-1)^{n+1+i}\xi^{(i)}_n. \quad (3.31)$$

Equation (3.26) with $m = -p$ is now the same as equation (3.26) with $m = p$, and likewise for (3.27) and (3.28). Therefore we can discard the equations with $m < 0$, and use (3.31) to substitute for $\xi^{(i)}_{-n}$ in terms of $\xi^{(i)}_n$, for each $n > 0$. The case where the irrotational component of the field is antisymmetric can be treated similarly.

4 Far field

The far field can be determined from (A.36), (A.45), (A.50), (A.55), (A.61), (A.66) and (A.69). If $0 \le \ell < k_1$ we can show that as $R \to \infty$, taking the upper sign if $x > 0$ and the

lower sign of $x < 0$,

$$\phi \sim C\mathrm{e}^{\mathrm{i}\alpha x}\mathrm{e}^{\beta_1 z} + M^{\pm}\mathrm{e}^{\pm\mathrm{i}\alpha x}\mathrm{e}^{\beta_1 z} + \mathcal{M}(\Theta)\sqrt{\frac{2}{\pi\kappa_1 R}}\,\mathrm{e}^{\mathrm{i}(\kappa_1 R-\pi/4)} + O(R^{-1}), \tag{4.1}$$

$$\psi \sim D_\psi\mathrm{e}^{\mathrm{i}\alpha x}\mathrm{e}^{\beta_2 z} + N^{\pm}\mathrm{e}^{\pm\mathrm{i}\alpha x}\mathrm{e}^{\beta_2 z} + \mathcal{N}(\Theta)\sqrt{\frac{2}{\pi\kappa_2 R}}\,\mathrm{e}^{\mathrm{i}(\kappa_2 R-\pi/4)} + O(R^{-3/4}), \tag{4.2}$$

$$\chi \sim D_\chi\mathrm{e}^{\mathrm{i}\alpha x}\mathrm{e}^{\beta_2 z} + L^{\pm}\mathrm{e}^{\pm\mathrm{i}\alpha x}\mathrm{e}^{\beta_2 z} + \mathcal{L}(\Theta)\sqrt{\frac{2}{\pi\kappa_2 R}}\,\mathrm{e}^{\mathrm{i}(\kappa_2 R-\pi/4)} + O(R^{-3/4}). \tag{4.3}$$

The total scattered field thus consists of a reflected Rayleigh wave, a transmitted Rayleigh wave, a cylindrical P-wave, and a cylindrical S-wave. If $k_1 < \ell < k_\mathrm{R}$, then κ_1 is imaginary and there is no scattered P-wave. If $k_2 < \ell < k_\mathrm{R}$ there is no scattered S-wave either. In terms of the incident wave angle this implies that for $0 \le \theta_\mathrm{inc} < \theta_1^*$, where $\sin\theta_1^* = k_1/k_\mathrm{R}$, the far field includes both P- and S- circular waves. For $\theta_1^* < \theta_\mathrm{inc} < \theta_2^*$, where $\sin\theta_2^* = k_2/k_\mathrm{R}$, the far field includes S-waves but not P-waves and for $\theta_2^* < \theta_\mathrm{inc} < \pi/2$ there are no circular waves at all. It is important to note that the critical angles θ_1^* and θ_2^* do not depend on frequency. This can be seen from (2.4) and (A.18) which show that linear relations exist between k_1, k_2 and k_R with the constants of proportionality depending only on Λ.

From (A.39), (A.46) and (A.51) we have

$$M^{\pm} = \sum_{n,i} \xi_n^{(i)} M_n^{(i)\pm} \tag{4.4}$$

$$= \frac{8}{\Delta'}\sum_{n=-\infty}^{\infty}(\pm 1)^n\left(-2\xi_n^{(1)}k_\mathrm{R}^2\beta_2\mathrm{e}^{-\beta_1 h}\mathrm{e}^{\mp n\zeta_1} + \mathrm{i}(k_\mathrm{R}^2+\beta_2^2)\mathrm{e}^{-\beta_2 h}\mathrm{e}^{\mp n\zeta_2}\left[\pm\alpha\xi_n^{(2)} - \xi_n^{(3)}\frac{\beta_2\ell}{k_2}\right]\right), \tag{4.5}$$

where Δ' is defined in (A.38). From (A.56), (A.62), (A.67), (A.70), and (A.71) we can show that, as expected,

$$N^{\pm} = \pm\frac{D_\psi}{C}M^{\pm}. \qquad L^{\pm} = \frac{D_\chi}{C}M^{\pm}. \tag{4.6}$$

Expressions for the cylindrical wave amplitudes can be obtained using the formulas given in the Appendix for the far-field forms of the multipoles. These are simplified if we write

$$\mathcal{S}_i = \frac{8\kappa_i\mathcal{G}_i\cos\Theta}{\Delta(\kappa_i\sin\Theta)}, \quad \mathcal{V}_i = \frac{4\cos\Theta}{\Delta(\kappa_i\sin\Theta)}(\nu^2 - 2\kappa_i^2\sin^2\Theta) \tag{4.7}$$

and

$$K_{ni}^{\pm} = (\pm\mathrm{i})^n\mathrm{e}^{\pm\mathrm{i}\kappa_i h\cos\Theta}\mathrm{e}^{\mp\mathrm{i}n\Theta}, \quad E_{ij} = \frac{\kappa_i\sin\Theta + \mathrm{i}\mathcal{G}_i}{\kappa_j}, \tag{4.8}$$

with $\mathcal{G}_1$ and $\mathcal{G}_2$ defined in (A.42) and (A.58), respectively. From (A.41), (A.47) and (A.52) we then have (for $0 \le \ell < k_1$)

$$\mathcal{M}(\Theta) = \sum_{n=-\infty}^{\infty}\Bigg(\xi_n^{(1)}\left[K_{n1}^- - K_{n1}^+ + (\kappa_1^2\sin^2\Theta + \ell^2)\mathcal{S}_1K_{n1}^+\right] - \left[\xi_n^{(2)}\kappa_1\sin\Theta + \xi_n^{(3)}\frac{\mathrm{i}\ell\mathcal{G}_1}{k_2}\right]\kappa_1\mathcal{V}_1E_{12}^n\mathrm{e}^{\mathrm{i}\mathcal{G}_1 h}\Bigg). \tag{4.9}$$

On the other hand, from (A.57), (A.63), (A.68), (A.72), (A.73) and (A.74), we have (for $0 \le \ell < k_2$)

$$\mathcal{N}(\Theta) = \sum_{n=-\infty}^{\infty} \Big(\xi_n^{(2)} \left(K_{n2}^- - K_{n2}^+ \right) + k_2 \sin\Theta \, \Xi_n \Big), \tag{4.10}$$

$$\mathcal{L}(\Theta) = \sum_{n=-\infty}^{\infty} \left(\xi_n^{(3)} \left(K_{n2}^- + K_{n2}^+ \right) + \mathrm{i}\ell \cos\Theta \, \Xi_n \right), \tag{4.11}$$

where

$$\Xi_n = \xi_n^{(1)} k_2 \mathcal{V}_2 E_{21}^n \mathrm{e}^{\mathrm{i}\mathcal{G}_2 h} + \mathcal{S}_2 K_{n2}^+ \left(\xi_n^{(2)} k_2 \sin\Theta + \xi_n^{(3)} \mathrm{i}\ell \cos\Theta \right). \tag{4.12}$$

The displacement field far from the cavity takes the form

$$\tilde{\mathbf{u}} \sim \mathrm{e}^{\mathrm{i}\alpha x} \left(C \mathrm{e}^{\beta_1 z} \mathbf{c}_+ + D \mathrm{e}^{\beta_2 z} \mathbf{d}_+ \right) + \frac{M^\pm}{C} \mathrm{e}^{-\mathrm{i}\alpha x} \left(C \mathrm{e}^{\beta_1 z} \mathbf{c}_\pm + D \mathrm{e}^{\beta_2 z} \mathbf{d}_\pm \right). \tag{4.13}$$

We thus define reflection and transmission coefficients, $\mathcal{R}$ and $\mathcal{T}$, via

$$\mathcal{R} = \frac{M^-}{C} = -\frac{N^-}{D_\psi} = \frac{L^-}{D_\chi}, \qquad \mathcal{T} = 1 + \frac{M^+}{C} = 1 + \frac{N^+}{D_\psi} = 1 + \frac{L^+}{D_\chi}, \tag{4.14}$$

which thus represent the amplitudes of the reflected and transmitted Rayleigh waves, respectively.

If we consider only the cylindrical waves then for large R we have (for the remainder of this section an overbar is used to denote the complex conjugate)

$$\begin{gathered} \tau_{rr}\overline{u_r} \sim \mu \left(-\nu^2 \phi - \frac{2\mathrm{i}\ell\kappa_2^2}{k_2} \chi \right) \left(-\mathrm{i}\kappa_1 \overline{\phi} - \frac{\ell \kappa_2}{k_2} \overline{\chi} \right), \quad \tau_{\theta r}\overline{u_\theta} \sim \mathrm{i}\mu\kappa_2^3 \psi \overline{\psi}, \\ \tau_{yr}\overline{u_y} \sim \mu \left(-2\ell\kappa_1 \phi + \frac{\mathrm{i}\nu^2 \kappa_2}{k_2} \chi \right) \left(-\mathrm{i}\ell \overline{\phi} + \frac{\kappa_2^2}{k_2} \overline{\chi} \right). \end{gathered} \tag{4.15}$$

Adding these and simplifying, we obtain

$$-\frac{\mathrm{i}}{\mu} \left(\tau_{rr}\overline{u_r} + \tau_{\theta r}\overline{u_\theta} + \tau_{yr}\overline{u_y} \right) \sim \kappa_1 k_2^2 |\phi|^2 + \kappa_2^3 (|\psi|^2 + |\chi|^2) + \frac{\mathrm{i}\ell\kappa_2}{k_2} (2\kappa_1\kappa_2 - \nu^2) \left(\overline{\phi}\chi + \phi\overline{\chi} \right). \tag{4.16}$$

If κ_1 and κ_2 are both real, so that there are both cylindrical P- and S-waves in the scattered field, we thus have

$$\begin{aligned} \mathrm{Re} \left(-\frac{\mathrm{i}}{\mu} \int_{-\pi/2}^{\pi/2} \left(\tau_{rr}\overline{u_r} + \tau_{\theta r}\overline{u_\theta} + \tau_{yr}\overline{u_y} \right) R \, \mathrm{d}\Theta \right) \\ \sim \frac{2}{\pi} \int_{-\pi/2}^{\pi/2} \left(k_2^2 |\mathcal{M}(\Theta)|^2 + \kappa_2^2 (|\mathcal{N}(\Theta)|^2 + |\mathcal{L}(\Theta)|^2) \right) \mathrm{d}\Theta. \end{aligned} \tag{4.17}$$

Conservation of energy for this problem is therefore equivalent to the identity

$$|\mathcal{R}|^2 + |\mathcal{T}|^2 + \frac{2}{\pi\alpha |C|^2 q} \int_{-\pi/2}^{\pi/2} \left(k_2^2 |\mathcal{M}(\Theta)|^2 + \kappa_2^2 (|\mathcal{N}(\Theta)|^2 + |\mathcal{L}(\Theta)|^2) \right) \mathrm{d}\Theta = 1, \tag{4.18}$$

where

$$\alpha|C|^2 q = \mathrm{Re}\left(-\frac{\mathrm{i}}{\mu}\int_{-\infty}^{0}\left(\tau_{11}^{\mathrm{inc}}\overline{u_1^{\mathrm{inc}}} + \tau_{21}^{\mathrm{inc}}\overline{u_2^{\mathrm{inc}}} + \tau_{31}^{\mathrm{inc}}\overline{u_3^{\mathrm{inc}}}\right)\mathrm{d}z\right). \tag{4.19}$$

This is the generalisation to oblique incidence of the energy relation for normal incidence given in [14, eqn. 68]. A long but straightforward calculation shows that

$$q = \frac{\beta_1}{2}\left(7 + \frac{k_{\mathrm{R}}^2}{\beta_2^2}\right) + \frac{k_2^2}{2\beta_1} - \frac{(k_{\mathrm{R}}^2 + \beta_2^2)}{\beta_2}\left(2 + \frac{k_2^2(\beta_2 - \beta_1) - 2k_1^2\beta_2}{2k_{\mathrm{R}}^2(\beta_1 + \beta_2)}\right). \tag{4.20}$$

Note that q does not depend on ℓ and that the formula for q in [14, eqn. 65] is incorrect.

5 Numerical Results

Clearly it is necessary to approximate numerically the integrals $A_{nm}^{(i)}$, $B_{nm}^{(i)}$ and $C_{nm}^{(i)}$, $i = 1, 2, 3$, which are defined in (A.26), (A.28) and (A.30). This turns out to be remarkably straightforward, given the complexity of the integrands. In each case, we deform the path of integration onto a smooth curve in the complex plane, and use a parametrisation of this curve to obtain an integral along the real line. There are two factors to consider in choosing an appropriate path: the rate at which the integrand converges toward zero as the integration variable moves away from the origin, and the distance from the path to the nearest singularity. For example, for an integral of the form

$$\mathrm{I} = \int_{-\infty}^{\infty} f(s)\mathrm{e}^{-\gamma_1 h}\,\mathrm{d}s \tag{5.1}$$

we can achieve steepest descent by using the path with the parametrisation

$$s(t) = t(t^2 - 2\mathrm{i}\kappa_1)^{1/2}, \quad -\infty < t < \infty, \tag{5.2}$$

since here the imaginary part of γ_1 is fixed. (It should be noted that the factors $\mathrm{e}^{\pm u_j}$ that occur in the integrands we need to compute are in fact algebraic functions, as can be seen from (A.21).) The range of integration is truncated at $|t| = R$, say, and computed using the composite trapezium rule. Assuming that the contributions from discarded parts of the integration range are negligible, the error in this approximation is then approximately proportional to $\mathrm{e}^{-\pi N\alpha/R}$, where N is the number of trapeziums used, and α is the perpendicular distance from the real line to the nearest singularity in the t-plane [25]. Thus there is a trade-off, in that a parametrisation other than (5.2) may require integration along a larger portion of the real axis, but the resulting increase in R may be outweighed by an increase in α, allowing fewer trapeziums to be used. In practice, we find that the choice of path need not be optimal; the convergence is extremely rapid for any reasonable choice.

Equations (3.26), (3.27) and (3.28) can be truncated by retaining terms with $|m| \le T$ and $|n| \le T$ in each and the three truncated systems can then be combined into a single $3(2T+1) \times 3(2T+1)$ linear system of equations. It is possible to use symmetry, as described at the end of §3, to reduce the size of this system but the additional complexity that this introduces into the equations coupled with the fact that our numerical scheme is very fast in any case means that this is of limited value. We have performed computations both ways to provide a check on our Fortran code but all the results presented were computed using the full system with $3(2T+1)$ unknowns. Double precision arithmetic was used throughout.

	a				
T	0.1	0.5	1.0	1.5	1.9
2	0.9996243045	0.8404633363	0.6656371353	0.6228537558	0.4985309784
3	0.9996242520	0.8382110935	0.5874433897	0.2233597972	0.2997736263
4	0.9996242521	0.8381217905	0.5805787388	0.3932954414	0.5254279448
5	0.9996242521	0.8381198430	0.5790500711	0.4567858981	0.6125161680
10	0.9996242521	0.8381198279	0.5789009157	0.4812591414	0.5111637852
15	0.9996242521	0.8381198279	0.5789009153	0.4812995516	0.5148693998
20	0.9996242521	0.8381198279	0.5789009153	0.4812995759	0.5225486968
25	0.9996242521	0.8381198279	0.5789009153	0.4812995759	0.5235483805
30	0.9996242521	0.8381198279	0.5789009153	0.4812995759	0.5236250726

Table 1: Modulus of the transmission coefficient $\mathcal{T}$ for the case where $\sigma = 0.2$, $k_2 = 1.5$, $h = 2.0$, and $\theta = 0.25$. Modes with $|m| \leq T$ and $|n| \leq T$ are retained in the field expansions.

All computations have been checked against the energy balance (4.18) and the errors caused by truncation and quadrature always amount to much less than 1% in the total energy. In each of the figures presented below, the value of T used in the calculations is stated and we have verified the results by computing them using a larger truncation value.

To reduce the number of parameters we have fixed $\sigma = 0.2$ throughout, which is a value representative of many rocks [26]. Our computations suggest that results are not particularly sensitive to the value of σ, which only enters the equations directly via (2.4). Note that $\sigma = 0.2$ corresponds to $\Lambda = 3/8$. To illustrate the convergence of our approach as T increases we present computed values of the modulus of the transmission coefficient $\mathcal{T}$ in Table 1. The two parameters which most significantly affect the convergence are the frequency and the gap between the cavity and the free surface. The frequency parameter used in the table is $k_2 = 1.5$ which is neither a low frequency (where the multipole method converges very quickly) or high frequency (where very little happens physically because the Rayleigh wave does not feel the presence of the cavity and passes over essentially unchanged). The cavity depth is $h = 2$ and we show results for five different cavity radii, ranging from 0.1 to 1.9, at which point the gap between the cavity and the free surface is small and we would expect the convergence to be less good. This is borne out by the numbers in the table, which show that the convergence improves as the gap between the cavity and the free surface increases. The table also demonstrates that except when the gap between the cavity and the free surface is small, we can expect to achieve very accurate results with moderate truncation sizes.

For normal incidence, Gregory [5] states a result for the reflection coefficient in the long-wave limit, by which we mean the limit $a \to 0$ for fixed frequency, in which case the submergence remains $O(1)$. Our numerical results do not fit with Gregory's expression, nor do our attempts to reproduce it analytically. We have calculated the leading-order behaviour of the unknowns $\xi_n^{(i)}$ in this limit and find, in agreement with Gregory, that $\xi_0^{(1)}$, $\xi_{\pm1}^{(i)}$, $\xi_{\pm2}^{(i)}$, $i = 1, 2$, are $O(a^2)$ whereas all the other coefficients (including $\xi_0^{(2)}$) are $O(a^4)$. However when we insert the leading order contributions to $\xi_n^{(i)}$ into the formula for $\mathcal{R}$, the result differs significantly (and is much more complicated than) Gregory's formula. Moreover, our

expression agrees with our numerical results in this limit. We find that, to leading order,

$$\xi_0^{(1)} \sim \frac{\mathrm{i}\pi a^2}{4}\left(k_2^2 - k_1^2\right) A_0^{\mathrm{inc}},$$
$$\xi_{\pm1}^{(1)} \sim \frac{\pi k_1 a^2}{8}\left(-\mathrm{i}k_1 A_{\pm1}^{\mathrm{inc}} \mp k_2 B_{\pm1}^{\mathrm{inc}}\right), \quad \xi_{\pm1}^{(2)} \sim \frac{\pi k_2 a^2}{8}\left(\pm k_1 A_{\pm1}^{\mathrm{inc}} - \mathrm{i}k_2 B_{\pm1}^{\mathrm{inc}}\right), \tag{5.3}$$
$$\xi_{\pm2}^{(1)} \sim \frac{\pi k_1^2 a^2}{4(k_2^2 - k_1^2)}\left(\mathrm{i}k_1^2 A_{\pm2}^{\mathrm{inc}} \pm k_2^2 B_{\pm2}^{\mathrm{inc}}\right), \quad \xi_{\pm2}^{(2)} \sim \frac{\pi k_2^2 a^2}{4(k_2^2 - k_1^2)}\left(\mp k_1^2 A_{\pm2}^{\mathrm{inc}} + \mathrm{i}k_2^2 B_{\pm2}^{\mathrm{inc}}\right).$$

We now present figures showing the proportion of the total scattered energy due to the longitudinal P-waves (the contribution to (4.18) from $\mathcal{M}$), the shear S-waves (the contribution to (4.18) from $\mathcal{N}$ and $\mathcal{L}$) and the reflected and transmitted Rayleigh waves (the contributions to (4.18) from $\mathcal{R}$ and $\mathcal{T}$, respectively.

Figures 1 and 2 show results for $a = 1$, $\sigma = 0.2$, against frequency, for three different values of θ_{inc}. Figure 1 is a case of a relatively deep cavity ($h = 2$) whereas in Figure 2 the cavity is much closer to the surface ($h = 1.3$). At low frequency we have long waves which are largely unaffected by the relatively small cavity and we find that $|\mathcal{T}| \to 1$ as $k_2 a \to 0$. At high frequency, the incident wave is tightly localised at the surface and we again find that $|\mathcal{T}|$ approaches 1 as $k_2 a$ increases. At head on incidence, there isn't much reflection and the contribution from the longitudinal P-wave is small. There is, however, a large range of frequencies for which the proportion of the incident wave energy that is converted into the S-wave is significant with a small range where this proportion is greater than 50%. For oblique incidence the picture becomes more complicated. For $\theta_{\mathrm{inc}} = \pi/4$ the picture is qualitatively the same as for head-on incidence but now there is no P-wave as this cuts off at $\theta_{\mathrm{inc}} = \arcsin(k_1/k_{\mathrm{R}}) \approx 0.188\pi$ and the amount of energy going into the S-wave now peaks at over 75%. For $\theta_{\mathrm{inc}} = 0.35\pi$ we see much stronger effects at the higher frequencies with large spikes in the S-wave energy around $k_2 a \approx 8.5$ and $k_2 a \approx 10.5$. Note that the S-wave cuts off at $\theta_{\mathrm{inc}} = \arcsin(k_2/k_{\mathrm{R}}) \approx 0.365\pi$. We can generate more interaction by moving the cavity closer to the surface and this is illustrated in Figure 2. There is now a much greater range of frequencies over which the incident wave energy is converted in significant proportions into reflected Rayleigh and scattered bulk waves.

Figures 3 and 4 show results for $a = 1$, $\sigma = 0.2$, against angle of incidence, for three different values of $k_2 a$. Figure 3 is a case of a relatively deep cavity ($h = 2$) whereas in Figure 4 the cavity is much closer to the surface ($h = 1.3$). The figures show the sharp (but continuous) cut off of the circular waves at $\theta_{\mathrm{inc}} \approx 0.188\pi$ and $\theta_{\mathrm{inc}} \approx 0.365\pi$. As θ increases, $|\mathcal{T}|$ starts to develop oscillations. Initially these are matched by oscillations in the contribution from the shear circular wave, but after this switches off there are strong oscillations in $|\mathcal{R}|$. These oscillations correspond to the region in which modes propagate along the surface of a cylindrical cavity in the absence of a free surface [22]. Calculations show that the spikes in the figures do not correspond precisely to the values of ℓ at which the modes occur, but in all cases there are a number of modes which occur for $\ell > k_2$, i.e. to the right of the second black square in the figures, with the mode with the largest value of ℓ corresponding closely to the last spike after which the curve becomes smoothly varying again. As $\theta \to \pi/2$, $\mathcal{R} \to -1$, cancelling the incident field (as usual for grazing incidence) and at high frequencies the incident wave is tightly localised to the surface, so not much happens until we get near to grazing. A key observation is that not much energy goes into the longitudinal P-wave at any frequency. Again, as shown in Figure 2 we generate more interaction by moving the cavity closer to the surface.

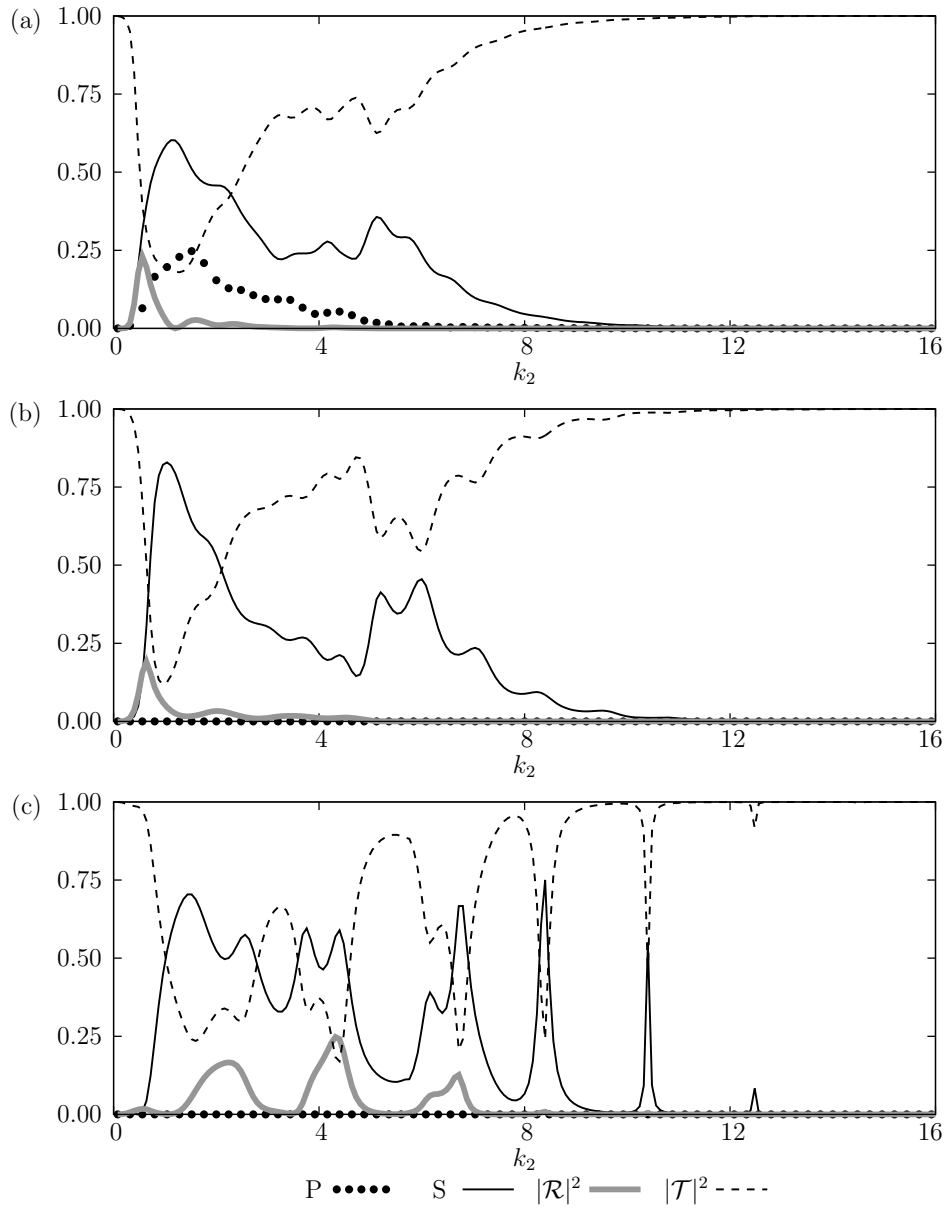

Figure 1: Proportion of scattered energy associated with P-, S-, reflected and transmitted waves when $a = 1$, $h = 2$, $\sigma = 0.2$, as a functions of frequency, with (a) $\theta_{\text{inc}} = 0$, (b) $\theta_{\text{inc}} = 0.25\pi$, (c) $\theta_{\text{inc}} = 0.35\pi$, computed with a truncation parameter $T = 15$.

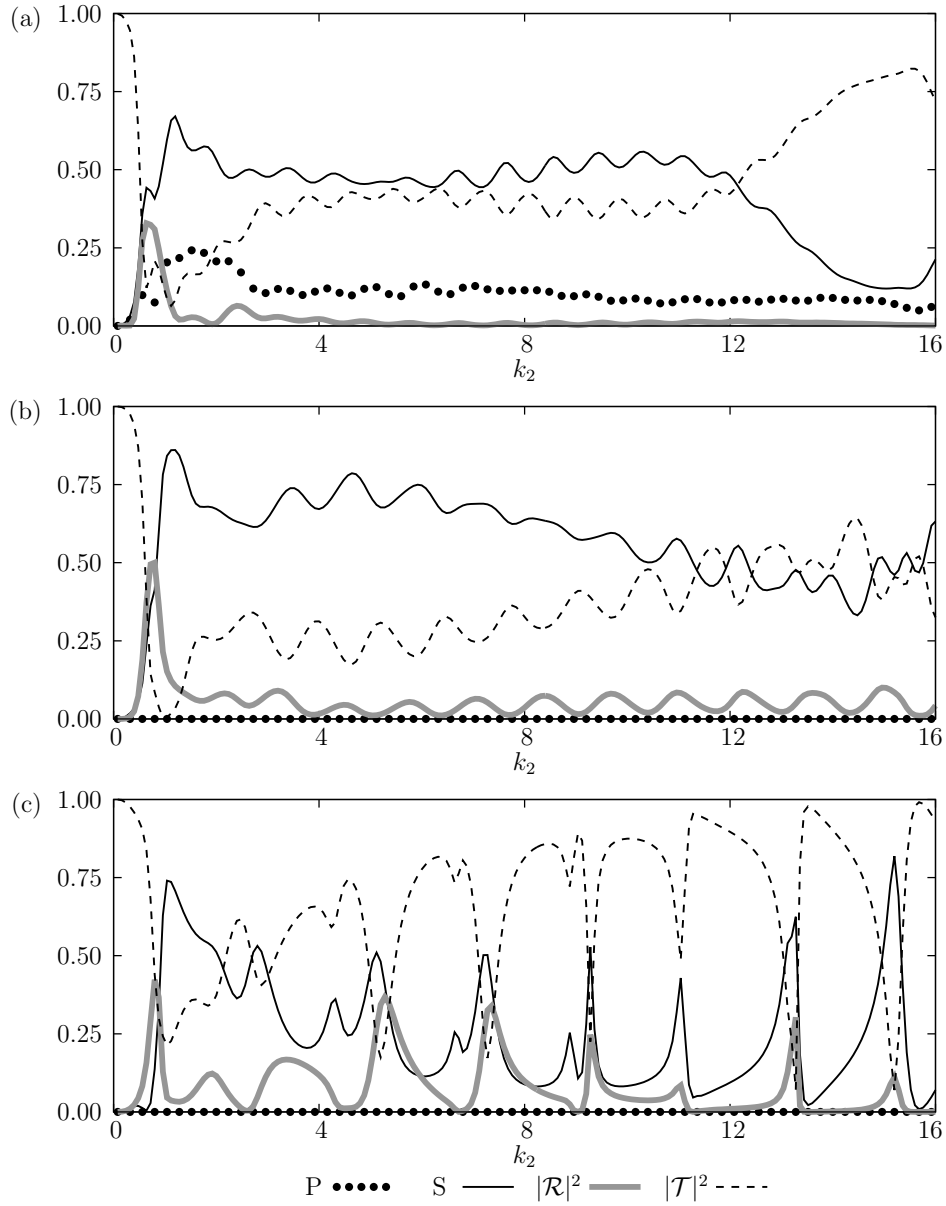

Figure 2: Proportion of scattered energy associated with P-, S-, reflected and transmitted waves when $a = 1$, $h = 1.3$, $\sigma = 0.2$, as a function of frequency, with (a) $\theta_{\text{inc}} = 0$, (b) $\theta_{\text{inc}} = 0.25\pi$, (c) $\theta_{\text{inc}} = 0.35\pi$. The curves for $\theta_{\text{inc}} = 0$ were computed with $T = 21$ whereas the other curves were computed with a truncation parameter $T = 15$.

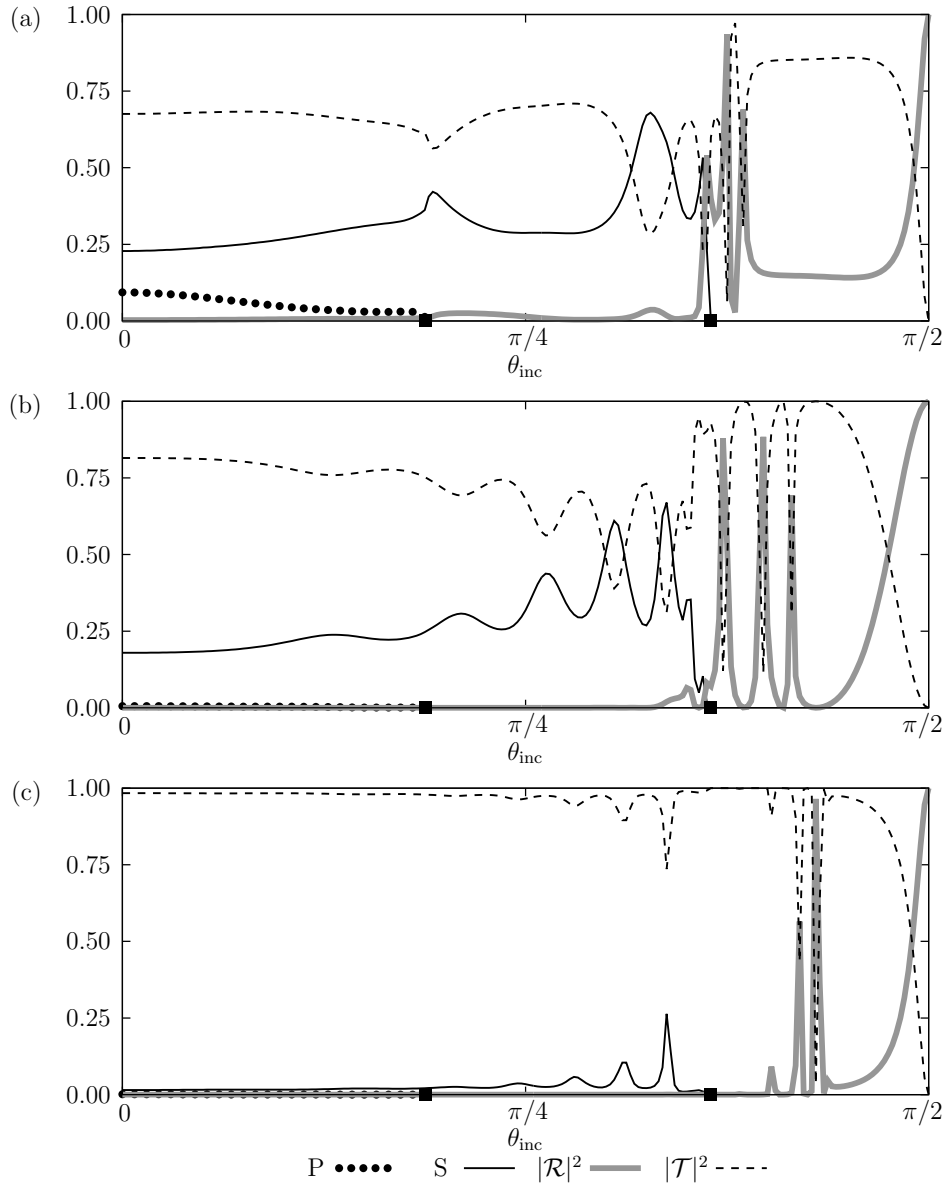

Figure 3: Proportion of scattered energy associated with P-, S-, reflected and transmitted waves when $a = 1$, $h = 2$, $\sigma = 0.2$, as a function of θ_{inc}, with (a) $k_2 a = \pi$, (b) $k_2 a = 2\pi$, (c) $k_2 a = 3\pi$, computed with truncation parameters $T = 8$, 10 and 12, respectively. The solid squares identify the critical angles $\theta_1^* \approx 0.188\pi$ and $\theta_2^* \approx 0.365\pi$.

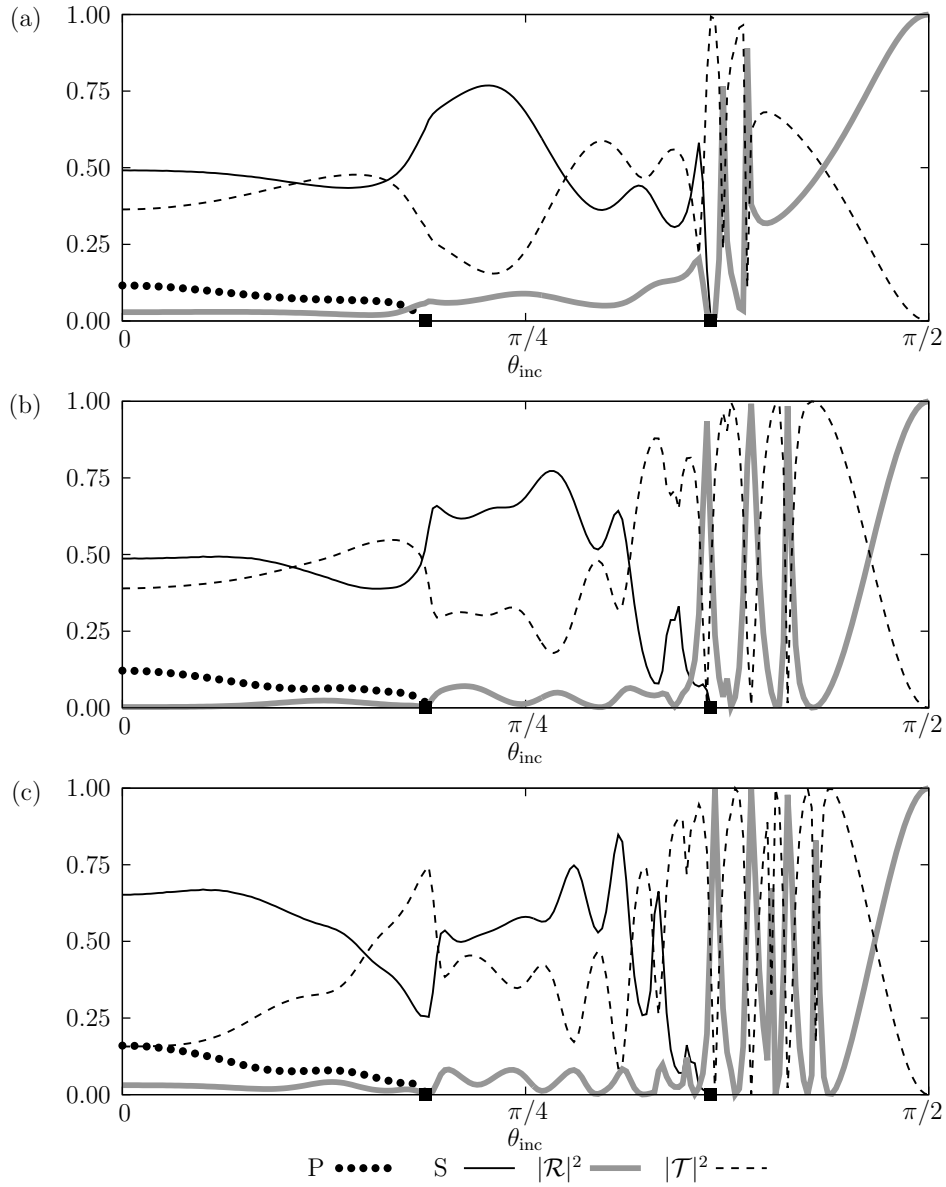

Figure 4: Proportion of scattered energy associated with P-, S-, reflected and transmitted waves when $a = 1$, $h = 1.3$, $\sigma = 0.2$, as a function of θ_{inc}, with (a) $k_2 a = \pi$, (b) $k_2 a = 2\pi$, (c) $k_2 a = 3\pi$, computed with truncation parameters $T = 8$, 10 and 12, respectively. The solid squares identify the critical angles $\theta_1^* \approx 0.188\pi$ and $\theta_2^* \approx 0.365\pi$.

A Mutipoles

The aim is to construct solutions to Navier's equation (2.1) which are (i) of the form $\mathbf{u} = \tilde{\mathbf{u}}(x,z)\mathrm{e}^{\mathrm{i}\ell y}$, (ii) singular at $z=-h$ ($h>0$), (iii) satisfy the condition of zero traction on $z=0$ and (iv) represent outgoing waves as $|x|\to\infty$. Singular solutions of the two-dimensional Helmholtz equation $(\nabla^2+k^2)u=0$ are given by

$$\mathrm{H}_n(kr)\mathrm{e}^{\mathrm{i}n\theta} = \frac{1}{\pi\mathrm{i}}\int_{-\infty}^{\infty}\mathrm{e}^{-k\gamma(t)|z+h|}\mathrm{e}^{\mathrm{i}kxt}(t-\gamma(t))^{n\,\mathrm{sgn}(z+h)}\frac{\mathrm{d}t}{\gamma(t)}, \tag{A.1}$$

where $\gamma(z)=(z^2-1)^{1/2}$ with branch cuts along along $(1,1+\mathrm{i}\infty)$ and $(-1,-1-\mathrm{i}\infty)$ and the path of integration is indented so as to pass above the branch point at $t=-1$ and below that at $t=1$ (see, for example, [27], but note that here $r\sin\theta=x$, $r\cos\theta=-(z+h)$). If we make the substitution $kt=s$ we obtain

$$\mathrm{H}_n(kr)\mathrm{e}^{\mathrm{i}n\theta} = \frac{1}{\pi\mathrm{i}k^{n\,\mathrm{sgn}(z+h)}}\int_{-\infty}^{\infty}\mathrm{e}^{-\tilde{\gamma}(s;k)|z+h|}\mathrm{e}^{\mathrm{i}sx}(s-\tilde{\gamma}(s;k))^{n\,\mathrm{sgn}(z+h)}\frac{\mathrm{d}s}{\tilde{\gamma}(s;k)}, \tag{A.2}$$

where $\tilde{\gamma}(s;k)=(s^2-k^2)^{1/2}$. This form is valid for non-zero complex k with the branch cuts as described above, provided $\mathrm{Re}\,\tilde{\gamma}>0$ as $|s|\to\infty$. In particular, it is valid for $k=\mathrm{i}q$, $q>0$, and we note that in this case the Hankel function becomes a modified Bessel function: $\mathrm{H}_n(\mathrm{i}qr)=(2/\pi\mathrm{i}^{n+1})\,\mathrm{K}_n(qr)$.

Provided $\kappa_1\neq 0$, multipoles $\tilde{\mathbf{u}}_n^{(i)}$ are triples $\{\phi_n^{(i)},\psi_n^{(i)},\chi_n^{(i)}\}$, $i=1,2,3$ of the form

$$\phi_n^{(1)} = \mathrm{H}_n(\kappa_1 r)\mathrm{e}^{\mathrm{i}n\theta} + \frac{1}{\pi\mathrm{i}\kappa_1^n}\int_{-\infty}^{\infty}A^{(1)}\mathrm{e}^{\gamma_1(z-h)}\mathrm{e}^{\mathrm{i}sx}(s-\gamma_1)^n\frac{\mathrm{d}s}{\gamma_1}, \tag{A.3}$$

$$= \frac{1}{\pi\mathrm{i}\kappa_1^n}\int_{-\infty}^{\infty}\left[\mathrm{e}^{-\gamma_1(z+h)}+A^{(1)}\mathrm{e}^{\gamma_1(z-h)}\right]\mathrm{e}^{\mathrm{i}sx}(s-\gamma_1)^n\frac{\mathrm{d}s}{\gamma_1}, \quad z>-h, \tag{A.4}$$

$$\psi_n^{(1)} = \frac{1}{\pi\mathrm{i}\kappa_1^n}\int_{-\infty}^{\infty}B^{(1)}\mathrm{e}^{-\gamma_1 h}\mathrm{e}^{\gamma_2 z}\mathrm{e}^{\mathrm{i}sx}(s-\gamma_1)^n\mathrm{d}s, \tag{A.5}$$

$$\chi_n^{(1)} = \frac{1}{\pi\mathrm{i}\kappa_1^n}\int_{-\infty}^{\infty}C^{(1)}\mathrm{e}^{-\gamma_1 h}\mathrm{e}^{\gamma_2 z}\mathrm{e}^{\mathrm{i}sx}(s-\gamma_1)^n\mathrm{d}s, \tag{A.6}$$

and provided $\kappa_2\neq 0$ we have

$$\phi_n^{(2)} = \frac{1}{\pi\mathrm{i}\kappa_2^n}\int_{-\infty}^{\infty}A^{(2)}\mathrm{e}^{-\gamma_2 h}\mathrm{e}^{\gamma_1 z}\mathrm{e}^{\mathrm{i}sx}(s-\gamma_2)^n\mathrm{d}s, \tag{A.7}$$

$$\psi_n^{(2)} = \mathrm{H}_n(\kappa_2 r)\mathrm{e}^{\mathrm{i}n\theta} + \frac{1}{\pi\mathrm{i}\kappa_2^n}\int_{-\infty}^{\infty}B^{(2)}\mathrm{e}^{\gamma_2(z-h)}\mathrm{e}^{\mathrm{i}sx}(s-\gamma_2)^n\frac{\mathrm{d}s}{\gamma_2}, \tag{A.8}$$

$$= \frac{1}{\pi\mathrm{i}\kappa_2^n}\int_{-\infty}^{\infty}\left[\mathrm{e}^{-\gamma_2(z+h)}+B^{(2)}\mathrm{e}^{\gamma_2(z-h)}\right]\mathrm{e}^{\mathrm{i}sx}(s-\gamma_2)^n\frac{\mathrm{d}s}{\gamma_2}, \quad z>-h, \tag{A.9}$$

$$\chi_n^{(2)} = \frac{1}{\pi\mathrm{i}\kappa_2^n}\int_{-\infty}^{\infty}C^{(2)}\mathrm{e}^{\gamma_2(z-h)}\mathrm{e}^{\mathrm{i}sx}(s-\gamma_2)^n\mathrm{d}s, \tag{A.10}$$

and

$$\phi_n^{(3)} = \frac{1}{\pi \mathrm{i} \kappa_2^n} \int_{-\infty}^{\infty} A^{(3)} \mathrm{e}^{-\gamma_2 h} \mathrm{e}^{\gamma_1 z} \mathrm{e}^{\mathrm{i}sx} (s-\gamma_2)^n \mathrm{d}s, \tag{A.11}$$

$$\psi_n^{(3)} = \frac{1}{\pi \mathrm{i} \kappa_2^n} \int_{-\infty}^{\infty} B^{(3)} \mathrm{e}^{\gamma_2 (z-h)} \mathrm{e}^{\mathrm{i}sx} (s-\gamma_2)^n \mathrm{d}s, \tag{A.12}$$

$$\chi_n^{(3)} = \mathrm{H}_n(\kappa_2 r) \mathrm{e}^{\mathrm{i}n\theta} + \frac{1}{\pi \mathrm{i} \kappa_2^n} \int_{-\infty}^{\infty} C^{(3)} \mathrm{e}^{\gamma_2 (z-h)} \mathrm{e}^{\mathrm{i}sx} (s-\gamma_2)^n \frac{\mathrm{d}s}{\gamma_2}, \tag{A.13}$$

$$= \frac{1}{\pi \mathrm{i} \kappa_2^n} \int_{-\infty}^{\infty} \left[\mathrm{e}^{-\gamma_2 (z+h)} + C^{(3)} \mathrm{e}^{\gamma_2 (z-h)} \right] \mathrm{e}^{\mathrm{i}sx} (s-\gamma_2)^n \frac{\mathrm{d}s}{\gamma_2}, \quad z > -h, \tag{A.14}$$

where $\gamma_i = \tilde{\gamma}(s;\kappa_i) = (s^2 - \kappa_i^2)^{1/2} = -\mathrm{i}(\kappa_i^2 - s^2)^{1/2}$. The precise interpretation of the contours will be determined once the functions $A^{(i)}$, $B^{(i)}$ and $C^{(i)}$ have been formally determined.

For the multipole triple $\{\phi_n^{(1)}, \psi_n^{(1)}, \chi_n^{(1)}\}$, application of the boundary conditions (2.19), (2.21) and (2.22) yields

$$\begin{aligned} A^{(1)} &= -\frac{1}{\Delta}((2\hat{s}^2 - k_2^2)^2 + 4\hat{s}^2 \gamma_1 \gamma_2) = -1 - \frac{8\hat{s}^2 \gamma_1 \gamma_2}{\Delta}, \\ B^{(1)} &= -\frac{4\mathrm{i}s k_2^2}{\kappa_2^2 \Delta}(2\hat{s}^2 - k_2^2), \quad C^{(1)} = \frac{4\mathrm{i}k_2 \gamma_2 \ell}{\kappa_2^2 \Delta}(2\hat{s}^2 - k_2^2), \end{aligned} \tag{A.15}$$

where we have written $\hat{s}^2 = s^2 + \ell^2$ and

$$\Delta = (2\hat{s}^2 - k_2^2)^2 - 4\hat{s}^2 \gamma_1 \gamma_2 = (2s^2 - \nu^2)^2 - 4\hat{s}^2 \gamma_1 \gamma_2. \tag{A.16}$$

Note that $A^{(1)}(s)$ and $C^{(1)}(s)$ are even functions, whereas $B^{(1)}(s)$ is an odd function. Since $\gamma_i^2 = \hat{s}^2 - k_i^2$, Δ is the secular determinant for Rayleigh waves with $\Delta = 0$ implying

$$(2\hat{s}^2 - k_2^2)^4 = 16\hat{s}^4 (\hat{s}^2 - k_1^2)(\hat{s}^2 - k_2^2), \tag{A.17}$$

which simplifies to the cubic

$$(k_2^2/\hat{s}^2)^3 - 8(k_2^2/\hat{s}^2)^2 + 8(k_2^2/\hat{s}^2)(3 - 2\Lambda) - 16(1 - \Lambda) = 0. \tag{A.18}$$

Only the real root (for $k_2^2/\hat{s}^2$) lying in $(0,1)$ is actually a solution to $\Delta = 0$ (the others, when they exist, correspond to taking different branches in the definition of γ_i). This leads to poles in the integrands at $\hat{s}^2 = k_{\mathrm{R}}^2$ or equivalently at $s = \pm(k_{\mathrm{R}}^2 - \ell^2)^{1/2} = \pm\alpha$. We choose the contour of integration to be indented above the pole at $s = -\alpha$ and below that at $s = \alpha$. This will ensure that the multipole behaves like an outgoing wave as $|x| \to \infty$.

Similarly for the multipole triple $\{\phi_n^{(2)}, \psi_n^{(2)}, \chi_n^{(2)}\}$

$$A^{(2)} = \frac{4\mathrm{i}s}{\Delta}(2\hat{s}^2 - k_2^2), \quad B^{(2)} = -1 - \frac{8\gamma_1 \gamma_2 k_2^2 s^2}{\kappa_2^2 \Delta}, \quad C^{(2)} = \frac{8\gamma_1 \gamma_2 \ell s k_2}{\kappa_2^2 \Delta}. \tag{A.19}$$

Note that $A^{(2)}(s)$ and $C^{(2)}(s)$ are odd functions, whereas $B^{(2)}(s)$ is an even function. Finally, for the triple $\{\phi_n^{(3)}, \psi_n^{(3)}, \chi_n^{(3)}\}$ we have

$$A^{(3)} = -\frac{4\mathrm{i}\gamma_2 \ell}{k_2 \Delta}(2\hat{s}^2 - k_2^2), \quad B^{(3)} = C^{(2)}, \quad C^{(3)} = 1 - \frac{8\gamma_1 \gamma_2^3 \ell^2}{\kappa_2^2 \Delta}. \tag{A.20}$$

Note that $A^{(3)}(s)$ and $C^{(3)}(s)$ are even functions, whereas $B^{(3)}(s)$ is an odd function.

Polar expansions of the multipoles can be obtained as follows: define u_i according to $s = \kappa_i \cosh u_i$, $\gamma_i = \kappa_i \sinh u_i$, i.e.,

$$\mathrm{e}^{u_i} = (s + \gamma_i)/\kappa_i, \qquad \mathrm{e}^{-u_i} = (s - \gamma_i)/\kappa_i. \tag{A.21}$$

In other words, if $\kappa_i = \mathrm{i}q_i$, $q_i > 0$, then

$$u_i = -\frac{\pi \mathrm{i}}{2} + \sinh^{-1} \frac{s}{q_i}. \tag{A.22}$$

On the other hand, if $\kappa_i > 0$ is real, then

$$u_i = \begin{cases} -\mathrm{i}\pi - \cosh^{-1} \frac{|s|}{\kappa_i}, & s < -\kappa_i, \\ -\mathrm{i} \cos^{-1} \frac{s}{\kappa_i}, & -\kappa_i < s < \kappa_i, \\ \cosh^{-1} \frac{s}{\kappa_i}, & s > \kappa_i. \end{cases} \tag{A.23}$$

In all cases we have $u_i(-s) = -\mathrm{i}\pi - u_i(s)$. Then, as in (3.14),

$$\mathrm{e}^{\gamma_i z} \mathrm{e}^{\mathrm{i}sx} = \mathrm{e}^{-\gamma_i h} \sum_{n=-\infty}^{\infty} \mathrm{J}_n(\kappa_i r) \mathrm{e}^{\mathrm{i}n\theta} \mathrm{e}^{-nu_i}. \tag{A.24}$$

Hence

$$\begin{gathered} \phi_n^{(1)} = \mathrm{H}_n(\kappa_1 r)\mathrm{e}^{\mathrm{i}n\theta} + \sum_{m=-\infty}^{\infty} A_{nm}^{(1)} \mathrm{J}_m(\kappa_1 r)\mathrm{e}^{\mathrm{i}m\theta}, \\ \psi_n^{(1)} = \sum_{m=-\infty}^{\infty} B_{nm}^{(1)} \mathrm{J}_m(\kappa_2 r)\mathrm{e}^{\mathrm{i}m\theta}, \quad \chi_n^{(1)} = \sum_{m=-\infty}^{\infty} C_{nm}^{(1)} \mathrm{J}_m(\kappa_2 r)\mathrm{e}^{\mathrm{i}m\theta}, \end{gathered} \tag{A.25}$$

where

$$\begin{gathered} A_{nm}^{(1)} = \frac{1}{\pi \mathrm{i}} \int_{-\infty}^{\infty} A^{(1)} \mathrm{e}^{-2\gamma_1 h} \mathrm{e}^{-(m+n)u_1} \frac{\mathrm{d}s}{\gamma_1}, \\ B_{nm}^{(1)} = \frac{1}{\pi \mathrm{i}} \int_{-\infty}^{\infty} B^{(1)} \mathrm{e}^{-(\gamma_1+\gamma_2)h} \mathrm{e}^{-mu_2 - nu_1} \mathrm{d}s, \quad C_{nm}^{(1)} = \frac{1}{\pi \mathrm{i}} \int_{-\infty}^{\infty} C^{(1)} \mathrm{e}^{-(\gamma_1+\gamma_2)h} \mathrm{e}^{-mu_2 - nu_1} \mathrm{d}s. \end{gathered} \tag{A.26}$$

For the multipole triple $\{\phi_n^{(2)}, \psi_n^{(2)}, \chi_n^{(2)}\}$ we have

$$\begin{gathered} \phi_n^{(2)} = \sum_{m=-\infty}^{\infty} A_{nm}^{(2)} \mathrm{J}_m(\kappa_1 r)\mathrm{e}^{\mathrm{i}m\theta}, \quad \chi_n^{(2)} = \sum_{m=-\infty}^{\infty} C_{nm}^{(2)} \mathrm{J}_m(\kappa_2 r)\mathrm{e}^{\mathrm{i}m\theta}, \\ \psi_n^{(2)} = \mathrm{H}_n(\kappa_2 r)\mathrm{e}^{\mathrm{i}n\theta} + \sum_{m=-\infty}^{\infty} B_{nm}^{(2)} \mathrm{J}_m(\kappa_2 r)\mathrm{e}^{\mathrm{i}m\theta}, \end{gathered} \tag{A.27}$$

where

$$\begin{gathered} A_{nm}^{(2)} = \frac{1}{\pi \mathrm{i}} \int_{-\infty}^{\infty} A^{(2)} \mathrm{e}^{-(\gamma_1+\gamma_2)h} \mathrm{e}^{-mu_1 - nu_2} \mathrm{d}s, \quad C_{nm}^{(2)} = \frac{1}{\pi \mathrm{i}} \int_{-\infty}^{\infty} C^{(2)} \mathrm{e}^{-2\gamma_2 h} \mathrm{e}^{-(m+n)u_2} \mathrm{d}s, \\ B_{nm}^{(2)} = \frac{1}{\pi \mathrm{i}} \int_{-\infty}^{\infty} B^{(2)} \mathrm{e}^{-2\gamma_2 h} \mathrm{e}^{-(m+n)u_2} \frac{\mathrm{d}s}{\gamma_2}, \end{gathered} \tag{A.28}$$

and for the triple $\{\phi_n^{(3)}, \psi_n^{(3)}, \chi_n^{(3)}\}$,

$$\begin{gathered}\phi_n^{(3)} = \sum_{m=-\infty}^{\infty} A_{nm}^{(3)}\, \mathrm{J}_m(\kappa_1 r)\mathrm{e}^{\mathrm{i}m\theta}, \quad \psi_n^{(3)} = \sum_{m=-\infty}^{\infty} B_{nm}^{(3)}\, \mathrm{J}_m(\kappa_2 r)\mathrm{e}^{\mathrm{i}m\theta}, \\ \chi_n^{(3)} = \mathrm{H}_n(\kappa_2 r)\mathrm{e}^{\mathrm{i}n\theta} + \sum_{m=-\infty}^{\infty} C_{nm}^{(3)}\, \mathrm{J}_m(\kappa_2 r)\mathrm{e}^{\mathrm{i}m\theta},\end{gathered} \tag{A.29}$$

where

$$\begin{gathered}A_{nm}^{(3)} = \frac{1}{\pi\mathrm{i}}\int_{-\infty}^{\infty} A^{(3)}\mathrm{e}^{-(\gamma_1+\gamma_2)h}\mathrm{e}^{-mu_1-nu_2}\mathrm{d}s, \quad B_{nm}^{(3)} = C_{nm}^{(2)}, \\ C_{nm}^{(3)} = \frac{1}{\pi\mathrm{i}}\int_{-\infty}^{\infty} C^{(3)}\mathrm{e}^{-2\gamma_2 h}\mathrm{e}^{-(m+n)u_2}\frac{\mathrm{d}s}{\gamma_2}.\end{gathered} \tag{A.30}$$

Note that changing s to $-s$ shows that

$$A_{nm}^{(i)} = (-1)^{n+m+i+1}A_{-n,-m}^{(i)}, \quad B_{nm}^{(i)} = (-1)^{n+m+i}B_{-n,-m}^{(i)}, \quad C_{nm}^{(i)} = (-1)^{n+m+i+1}C_{-n,-m}^{(i)}. \tag{A.31}$$

Far field

We wish to determine the asymptotic behaviour of the multipoles as $R \to \infty$, uniformly in Θ, where R and Θ are polar coordinates centred at the origin, i.e. $x = R\sin\Theta$, $z = -R\cos\Theta$. Note that

$$r = R - h\cos\Theta + O(R^{-1}), \qquad \theta = \Theta + O(R^{-1}). \tag{A.32}$$

We have, from (A.3) and (A.15),

$$\phi_n^{(1)} = \mathrm{H}_n(\kappa_1 r)\mathrm{e}^{\mathrm{i}n\theta} - \frac{1}{\pi\mathrm{i}\kappa_1^n}\int_{-\infty}^{\infty}\left(1 + \frac{8\hat{s}^2\gamma_1\gamma_2}{\Delta(s)}\right)\mathrm{e}^{\gamma_1(z-h)}\mathrm{e}^{\mathrm{i}sx}(s-\gamma_1)^n\frac{\mathrm{d}s}{\gamma_1}, \tag{A.33}$$

$$= \mathrm{H}_n(\kappa_1 r)\mathrm{e}^{\mathrm{i}n\theta} - \frac{1}{\pi\mathrm{i}}\int_{-\infty}^{\infty}\left(1 + \frac{8\kappa_1(\kappa_1^2 t^2 + \ell^2)\gamma_2(\kappa_1 t)\gamma}{\Delta(\kappa_1 t)}\right)\mathrm{e}^{-2\kappa_1 h\gamma}\mathrm{e}^{\kappa_1 r g(t)}(t-\gamma)^n\frac{\mathrm{d}t}{\gamma}, \tag{A.34}$$

where

$$g(t) = -\gamma(t)\cos\theta + \mathrm{i}t\sin\theta. \tag{A.35}$$

The asymptotics as $R \to \infty$ can readily be determined as shown in detail for the case of normal incidence in [4]. The leading order behaviour comes from two contributions: from the poles on the real axis (which are most easily calculated from (A.33)) and from the saddle point corresponding to the root of $g'(t) = 0$ (which can be deduced from (A.34)). In fact

$$\phi_n^{(1)} \sim M_n^{(1)\pm}\mathrm{e}^{\pm\mathrm{i}\alpha x}\mathrm{e}^{\beta_1 z} + \mathcal{M}_n^{(1)}(\Theta)\sqrt{\frac{2}{\pi\kappa_1 R}}\,\mathrm{e}^{\mathrm{i}(\kappa_1 R - \pi/4)} + O(R^{-1}), \tag{A.36}$$

where the upper sign is to be taken if $x > 0$ and the lower sign if $x < 0$. If $\kappa_1^2 < 0$, the saddle point contribution is exponentially small.

To determine $M_n^{(1)\pm}$ we note that the poles are at $s = \pm\alpha$, at which points

$$\hat{s} = k_{\mathrm{R}}, \quad \gamma_i = \beta_i, \quad 2\hat{s}^2 - k_2^2 = k_{\mathrm{R}}^2 + \beta_2^2 = 2k_{\mathrm{R}}\sqrt{\beta_1\beta_2}. \tag{A.37}$$

We define

$$\Delta' = \frac{\mathrm{d}\Delta}{\mathrm{d}s}\Big|_{s=\alpha} = -\frac{\mathrm{d}\Delta}{\mathrm{d}s}\Big|_{s=-\alpha} = \frac{4\alpha}{\beta_1\beta_2}(\beta_2-\beta_1)\left(k_{\mathrm{R}}^2(\beta_1-\beta_2)+2\beta_1\beta_2^2\right) \tag{A.38}$$

and note that this cannot vanish since $\beta_1 > \beta_2 > 0$. When $x > 0$ the contributing pole is at $s = \alpha$, whereas when $x < 0$ it is the pole at $s = -\alpha$ that contributes. Thus, from (A.33) and (3.11),

$$M_n^{(1)\pm} = -\frac{16k_{\mathrm{R}}^2\beta_2}{\Delta'}\mathrm{e}^{-\beta_1 h}\left(\frac{\pm\alpha-\beta_1}{\kappa_1}\right)^n = -(\pm 1)^n\frac{16k_{\mathrm{R}}^2\beta_2}{\Delta'}\mathrm{e}^{-\beta_1 h}\mathrm{e}^{\mp n\zeta_1}. \tag{A.39}$$

To determine $\mathcal{M}_n^{(1)}(\Theta)$ we first note that $g'(t) = 0$ if and only if $t = t^* = \sin\theta$ and that

$$\gamma(t^*) = -\mathrm{i}\cos\theta, \qquad g(t^*) = \mathrm{i}, \qquad g''(t^*) = -\mathrm{i}/\cos^2\theta. \tag{A.40}$$

The two steepest descent contours from the saddle point make angles $-\pi/4$ and $3\pi/4$ with the positive x-axis and hence if we deform the contour of integration into the path of steepest descent we can then calculate the contribution from the saddle point using the expression [28, eqn. 7.2.10]

$$f(t^*)\mathrm{e}^{\kappa_1 r g(t^*)}\mathrm{e}^{-\mathrm{i}\pi/4}\sqrt{\frac{2\pi}{\kappa_1 r|g''(t^*)|}}.$$

There is also a contribution from the Hankel function. Thus, from (A.34) using (A.32),

$$\mathcal{M}_n^{(1)}(\Theta) = (-\mathrm{i})^n\mathrm{e}^{-\mathrm{i}\kappa_1 h\cos\Theta}\mathrm{e}^{\mathrm{i}n\Theta} + \left(\frac{8\kappa_1\mathcal{G}_1(\kappa_1^2\sin^2\Theta+\ell^2)\cos\Theta}{\Delta(\kappa_1\sin\Theta)}-1\right)\mathrm{i}^n\mathrm{e}^{\mathrm{i}\kappa_1 h\cos\Theta}\mathrm{e}^{-\mathrm{i}n\Theta}, \tag{A.41}$$

where

$$\mathcal{G}_1 = \mathrm{i}\gamma_2(\kappa_1\sin\Theta) = \mathrm{i}(\kappa_1^2\sin^2\Theta-\kappa_2^2)^{1/2} = (\kappa_2^2-\kappa_1^2\sin^2\Theta)^{1/2}. \tag{A.42}$$

For $\phi_n^{(2)}$ we have, from (A.7) and (A.19),

$$\phi_n^{(2)} = \frac{4}{\pi\kappa_2^n}\int_{-\infty}^{\infty}\frac{s}{\Delta}(2\hat{s}^2-k_2^2)\mathrm{e}^{-\gamma_2 h}\mathrm{e}^{\gamma_1 z}\mathrm{e}^{\mathrm{i}sx}(s-\gamma_2)^n\mathrm{d}s \tag{A.43}$$

$$= \frac{4\kappa_1}{\pi\kappa_2^n}\int_{-\infty}^{\infty}\frac{\kappa_1 t}{\Delta(\kappa_1 t)}(2\kappa_1^2t^2-\nu^2)\mathrm{e}^{-(\kappa_1\gamma+\gamma_2(\kappa_1 t))h}\mathrm{e}^{\kappa_1 r g(t)}(\kappa_1 t-\gamma_2(\kappa_1 t))^n\mathrm{d}t \tag{A.44}$$

and hence

$$\phi_n^{(2)} \sim M_n^{(2)\pm}\mathrm{e}^{\pm\mathrm{i}\alpha x}\mathrm{e}^{\beta_1 z} + \mathcal{M}_n^{(2)}(\Theta)\sqrt{\frac{2}{\pi\kappa_1 R}}\,\mathrm{e}^{\mathrm{i}(\kappa_1 R-\pi/4)} + O(R^{-1}), \tag{A.45}$$

with

$$M_n^{(2)\pm} = (\pm 1)^{n+1}\frac{8\mathrm{i}\alpha}{\Delta'}(k_{\mathrm{R}}^2+\beta_2^2)\mathrm{e}^{-\beta_2 h}\mathrm{e}^{\mp n\zeta_2} \tag{A.46}$$

and

$$\mathcal{M}_n^{(2)}(\Theta) = \frac{4\kappa_1^2\sin\Theta\cos\Theta}{\Delta(\kappa_1\sin\Theta)}(2\kappa_1^2\sin^2\Theta-\nu^2)\mathrm{e}^{\mathrm{i}\mathcal{G}_1 h}\left(\frac{\kappa_1\sin\Theta+\mathrm{i}\mathcal{G}_1}{\kappa_2}\right)^n. \tag{A.47}$$

If $\kappa_1^2 < 0$, the saddle point contribution is exponentially small.

For $\phi_n^{(3)}$ we have, from (A.11) and (A.20),

$$\phi_n^{(3)} = -\frac{4\ell}{\pi\kappa_2^n}\int_{-\infty}^{\infty}\frac{\gamma_2}{k_2\Delta}(2\hat{s}^2-k_2^2)\mathrm{e}^{-\gamma_2 h}\mathrm{e}^{\gamma_1 z}\mathrm{e}^{\mathrm{i}sx}(s-\gamma_2)^n\mathrm{d}s \tag{A.48}$$

$$= -\frac{4\ell\kappa_1}{\pi\kappa_2^n}\int_{-\infty}^{\infty}\frac{\gamma_2(\kappa_1 t)}{k_2\Delta(\kappa_1 t)}(2\kappa_1^2t^2-\nu^2)\mathrm{e}^{-(\kappa_1\gamma+\gamma_2(\kappa_1 t))h}\mathrm{e}^{\kappa_1 r g(t)}(\kappa_1 t-\gamma_2(\kappa_1 t))^n\mathrm{d}t \tag{A.49}$$

and hence

$$\phi_n^{(3)} \sim M_n^{(3)\pm}\mathrm{e}^{\pm\mathrm{i}\alpha x}\mathrm{e}^{\beta_1 z} + \mathcal{M}_n^{(3)}(\Theta)\sqrt{\frac{2}{\pi\kappa_1 R}}\,\mathrm{e}^{\mathrm{i}(\kappa_1 R-\pi/4)} + O(R^{-1}), \tag{A.50}$$

with

$$M_n^{(3)\pm} = -(\pm 1)^n\frac{8\mathrm{i}\beta_2\ell}{k_2\Delta'}(k_{\mathrm{R}}^2+\beta_2^2)\mathrm{e}^{-\beta_2 h}\mathrm{e}^{\mp n\zeta_2} \tag{A.51}$$

and

$$\mathcal{M}_n^{(3)}(\Theta) = \frac{4\mathrm{i}\ell\kappa_1\mathcal{G}_1\cos\Theta}{k_2\Delta(\kappa_1\sin\Theta)}(2\kappa_1^2\sin^2\Theta-\nu^2)\mathrm{e}^{\mathrm{i}\mathcal{G}_1 h}\left(\frac{\kappa_1\sin\Theta+\mathrm{i}\mathcal{G}_1}{\kappa_2}\right)^n. \tag{A.52}$$

If $\kappa_1^2 < 0$, the saddle point contribution is exponentially small.

For $\psi_n^{(i)}$ and $\chi_n^{(i)}$ there is an additional complication due to the fact that the saddle point at $s=\kappa_2\sin\theta$ can coincide with the branch point at $s=\kappa_1$. However, as shown in [4] the only consequence of this is that the error term becomes $O(R^{-3/4})$ rather than $O(R^{-1})$. Thus for $\psi_n^{(1)}$ we have, from (A.5) and (A.15),

$$\psi_n^{(1)} = -\frac{4k_2^2}{\pi\kappa_2^2\kappa_1^n}\int_{-\infty}^{\infty}\frac{s}{\Delta}(2\hat{s}^2-k_2^2)\mathrm{e}^{-\gamma_1 h}\mathrm{e}^{\gamma_2 z}\mathrm{e}^{\mathrm{i}sx}(s-\gamma_1)^n\mathrm{d}s \tag{A.53}$$

$$= -\frac{4k_2^2}{\pi\kappa_1^n}\int_{-\infty}^{\infty}\frac{t(2\kappa_2^2t^2-\nu^2)}{\Delta(\kappa_2 t)}\mathrm{e}^{-(\kappa_2\gamma+\gamma_1(\kappa_2 t))h}\mathrm{e}^{\kappa_2 r g(t)}(\kappa_2 t-\gamma_1(\kappa_2 t))^n\mathrm{d}t \tag{A.54}$$

and hence

$$\psi_n^{(1)} \sim N_n^{(1)\pm}\mathrm{e}^{\pm\mathrm{i}\alpha x}\mathrm{e}^{\beta_2 z} + \mathcal{N}_n^{(1)}(\Theta)\sqrt{\frac{2}{\pi\kappa_2 R}}\,\mathrm{e}^{\mathrm{i}(\kappa_2 R-\pi/4)} + O(R^{-3/4}), \tag{A.55}$$

with

$$N_n^{(1)\pm} = -(\pm 1)^{n+1}\frac{8\mathrm{i}\alpha k_2^2}{\kappa_2^2\Delta'}(k_{\mathrm{R}}^2+\beta_2^2)\mathrm{e}^{-\beta_1 h}\mathrm{e}^{\mp n\zeta_1} \tag{A.56}$$

and

$$\mathcal{N}_n^{(1)}(\Theta) = \frac{4k_2^2\sin\Theta\cos\Theta(\nu^2-2\kappa_2^2\sin^2\Theta)}{\Delta(\kappa_2\sin\Theta)}\mathrm{e}^{\mathrm{i}\mathcal{G}_2 h}\left(\frac{\kappa_2\sin\Theta+\mathrm{i}\mathcal{G}_2}{\kappa_1}\right)^n, \tag{A.57}$$

where

$$\mathcal{G}_2 = \mathrm{i}\gamma_1(\kappa_2\sin\Theta) = \mathrm{i}(\kappa_2^2\sin^2\Theta-\kappa_1^2)^{1/2} = (\kappa_1^2-\kappa_2^2\sin^2\Theta)^{1/2}. \tag{A.58}$$

For $\psi_n^{(2)}$ we have, from (A.8) and (A.19),

$$\psi_n^{(2)} = \mathrm{H}_n(\kappa_2 r)\mathrm{e}^{\mathrm{i}n\theta} - \frac{1}{\pi\mathrm{i}\kappa_2^n}\int_{-\infty}^{\infty}\left(1+\frac{8\gamma_1\gamma_2k_2^2s^2}{\kappa_2^2\Delta}\right)\mathrm{e}^{\gamma_2(z-h)}\mathrm{e}^{\mathrm{i}sx}(s-\gamma_2)^n\frac{\mathrm{d}s}{\gamma_2} \tag{A.59}$$

$$= \mathrm{H}_n(\kappa_2 r)\mathrm{e}^{\mathrm{i}n\theta} - \frac{1}{\pi\mathrm{i}}\int_{-\infty}^{\infty}\left(1+\frac{8\gamma_1(\kappa_2 t)\gamma\kappa_2k_2^2t^2}{\Delta}\right)\mathrm{e}^{-2\kappa_2 h\gamma}\mathrm{e}^{\kappa_2 r g(t)}(t-\gamma)^n\frac{\mathrm{d}t}{\gamma} \tag{A.60}$$

and so

$$\psi_n^{(2)} \sim N_n^{(2)\pm} \mathrm{e}^{\pm \mathrm{i}\alpha x} \mathrm{e}^{\beta_2 z} + \mathcal{N}_n^{(2)}(\Theta) \sqrt{\frac{2}{\pi \kappa_2 R}}\, \mathrm{e}^{\mathrm{i}(\kappa_2 R - \pi/4)} + O(R^{-3/4}), \tag{A.61}$$

with

$$N_n^{(2)\pm} = -(\pm 1)^n \frac{16 \beta_1 k_2^2 \alpha^2}{\kappa_2^2 \Delta'} \mathrm{e}^{-\beta_2 h} \mathrm{e}^{\mp n \zeta_2} \tag{A.62}$$

and

$$\mathcal{N}_n^{(2)}(\Theta) = (-\mathrm{i})^n \mathrm{e}^{-\mathrm{i}\kappa_2 h \cos\Theta} \mathrm{e}^{\mathrm{i}n\Theta} + \left(\frac{8 \mathcal{G}_2 \kappa_2 k_2^2 \sin^2\Theta \cos\Theta}{\Delta(\kappa_2 \sin\Theta)} - 1 \right) \mathrm{i}^n \mathrm{e}^{\mathrm{i}\kappa_2 h \cos\Theta} \mathrm{e}^{-\mathrm{i}n\Theta}. \tag{A.63}$$

For $\psi_n^{(3)}$ we have, from (A.12) and (A.20),

$$\psi_n^{(3)} = \frac{8 \ell k_2}{\pi \mathrm{i} \kappa_2^{n+2}} \int_{-\infty}^{\infty} \frac{\gamma_1 \gamma_2 s}{\Delta} \mathrm{e}^{\gamma_2 (z-h)} \mathrm{e}^{\mathrm{i}sx} (s - \gamma_2)^n \mathrm{d}s \tag{A.64}$$

$$= \frac{8 \ell k_2 \kappa_2}{\pi \mathrm{i}} \int_{-\infty}^{\infty} \frac{\gamma_1(\kappa_2 t) \gamma t}{\Delta(\kappa_2 t)} \mathrm{e}^{-2\kappa_2 \gamma h} \mathrm{e}^{\kappa_2 r g(t)} (t - \gamma)^n \mathrm{d}t \tag{A.65}$$

and so

$$\psi_n^{(3)} \sim N_n^{(3)\pm} \mathrm{e}^{\pm \mathrm{i}\alpha x} \mathrm{e}^{\beta_2 z} + \mathcal{N}_n^{(3)}(\Theta) \sqrt{\frac{2}{\pi \kappa_2 R}}\, \mathrm{e}^{\mathrm{i}(\kappa_2 R - \pi/4)} + O(R^{-3/4}), \tag{A.66}$$

with

$$N_n^{(3)\pm} = (\pm 1)^{n+1} \frac{16 \ell k_2 \beta_1 \beta_2 \alpha}{\kappa_2^2 \Delta'} \mathrm{e}^{-\beta_2 h} \mathrm{e}^{\mp n \zeta_2} \tag{A.67}$$

and

$$\mathcal{N}_n^{(3)}(\Theta) = \frac{8 \mathrm{i} \ell k_2 \kappa_2 \mathcal{G}_2 \sin\Theta \cos^2\Theta}{\Delta(\kappa_2 \sin\Theta)} \mathrm{i}^n \mathrm{e}^{\mathrm{i}\kappa_2 h \cos\Theta} \mathrm{e}^{-\mathrm{i}n\Theta}. \tag{A.68}$$

In a similar way we can show that

$$\chi_n^{(i)} \sim L_n^{(i)\pm} \mathrm{e}^{\pm \mathrm{i}\alpha x} \mathrm{e}^{\beta_2 z} + \mathcal{L}_n^{(i)}(\Theta) \sqrt{\frac{2}{\pi \kappa_2 R}}\, \mathrm{e}^{\mathrm{i}(\kappa_2 R - \pi/4)} + O(R^{-3/4}), \tag{A.69}$$

with

$$L_n^{(1)\pm} = (\pm 1)^n \frac{8 \mathrm{i} k_2 \ell \beta_2}{\kappa_2^2 \Delta'} (k_{\mathrm{R}}^2 + \beta_2^2) \mathrm{e}^{-\beta_1 h} \mathrm{e}^{\mp n \zeta_1}, \tag{A.70}$$

$$L_n^{(2)\pm} = (\pm 1)^{n+1} \frac{16 \ell k_2 \beta_1 \beta_2 \alpha}{\kappa_2^2 \Delta'} \mathrm{e}^{-\beta_2 h} \mathrm{e}^{\mp n \zeta_2}, \quad L_n^{(3)\pm} = L_n^{(2)\pm} \frac{\ell \beta_2}{k_2 \alpha}, \tag{A.71}$$

and

$$\mathcal{L}_n^{(1)}(\Theta) = -\frac{4 \mathrm{i} k_2 \ell \cos^2\Theta}{\Delta(\kappa_2 \sin\Theta)} (2\kappa_2^2 \sin^2\Theta - \nu^2) \mathrm{e}^{\mathrm{i}\mathcal{G}_2 h} \left(\frac{\kappa_2 \sin\Theta + \mathrm{i}\mathcal{G}_2}{\kappa_1} \right)^n, \tag{A.72}$$

$$\mathcal{L}_n^{(2)}(\Theta) = \frac{8 \mathrm{i} \ell k_2 \kappa_2 \mathcal{G}_2 \sin\Theta \cos^2\Theta}{\Delta(\kappa_2 \sin\Theta)} \mathrm{i}^n \mathrm{e}^{\mathrm{i}\kappa_2 h \cos\Theta} \mathrm{e}^{-\mathrm{i}n\Theta}, \tag{A.73}$$

$$\mathcal{L}_n^{(3)}(\Theta) = (-\mathrm{i})^n \mathrm{e}^{-\mathrm{i}\kappa_2 h \cos\Theta} \mathrm{e}^{\mathrm{i}n\Theta} + \left(1 - \frac{8 \kappa_2 \mathcal{G}_2 \ell^2 \cos^3\Theta}{\Delta(\kappa_2 \sin\Theta)} \right) \mathrm{i}^n \mathrm{e}^{\mathrm{i}\kappa_2 h \cos\Theta} \mathrm{e}^{-\mathrm{i}n\Theta}. \tag{A.74}$$

If $\kappa_2^2 < 0$, the saddle point contributions in $\psi_n^{(i)}$ and $\chi_n^{(i)}$ are exponentially small.

The limits $\kappa_1 \to 0$ and $\kappa_2 \to 0$

Many equations in this paper include terms that do not exist in the limits $\kappa_1 \to 0$ and $\kappa_2 \to 0$. To show that our method remains valid in these cases, we introduce scaled coefficients into (3.16), via

$$\xi_n^{(1)} = \kappa_1^{|n|}\tilde{\xi}_n^{(1)}, \quad \text{and} \quad \xi_n^{(j)} = \kappa_2^{|n|}\tilde{\xi}_n^{(j)}, \quad j = 2, 3. \tag{A.75}$$

To verify that these scalings are correct, we must show that all singularities in the far field and in the coefficients of the linear system formed from (3.26)–(3.28) are now removable. The definitions of the functions $A^{(j)}$, $B^{(j)}$ and $C^{(j)}$ remain valid as $\kappa_1 \to 0$, but the function γ_1 appears in the denominator in (A.3) and this could potentially introduce a singularity that is not removable. However, using (A.15), we can write

$$\phi_n^{(1)} = \mathrm{H}_n(\kappa_1 r)\mathrm{e}^{\mathrm{i}n\theta} - \mathrm{H}_n(\kappa_1 \tilde{r})\mathrm{e}^{\mathrm{i}n\tilde{\theta}} - \frac{8}{\pi \mathrm{i}\kappa_1^n}\int_{-\infty}^{\infty} \frac{\hat{s}^2\gamma_2}{\Delta}\mathrm{e}^{-\gamma_1(h-z)}\mathrm{e}^{\mathrm{i}sx}(s-\gamma_1)^n \,\mathrm{d}s, \tag{A.76}$$

where the polar coordinate system $(\tilde{r}, \tilde{\theta})$ is centred at the point $(0, h)$, so that $\tilde{r}\sin\tilde{\theta} = x$ and $\tilde{r}\cos\tilde{\theta} = h - z$. Evidently the integral in (A.76) remains bounded in the limit $\kappa_1 \to 0$, if $n \geq 0$. If $n < 0$, we rewrite it using the identity

$$\frac{s-\gamma_1}{\kappa_1} = \frac{\kappa_1}{s+\gamma_1}. \tag{A.77}$$

We can then use [29, eqn. 10.7.7] to show that $\phi_n^{(1)} = O(\kappa_1^{-|n|})$ if $n \neq 0$. On the other hand, if $n = 0$ then the integral poses no problem, and we can take the limit $\kappa_1 \to 0$ using [29, eqn. 10.7.2].

With the coefficients scaled as in (A.75), the only potentially singular term in the linear system formed from (3.26)–(3.28) is

$$T = -\bar{\nu}^2\xi_0^{(1)}\big(H_{01} + A_{00}^{(1)}J_{01}\big), \tag{A.78}$$

from (3.26) with $m = 0$. However, using (A.15), we can write $A_{00}^{(1)}$ from (A.26) with $m = n = 0$ in the form

$$A_{00}^{(1)} = -\,\mathrm{H}_0(2\kappa_1 h) - \frac{8}{\pi\mathrm{i}}\int_{-\infty}^{\infty}\frac{\hat{s}^2\gamma_2}{\Delta}\,\mathrm{e}^{-2\gamma_1 h}\,\mathrm{d}s, \tag{A.79}$$

which shows that T is regular in the limit $\kappa_1 \to 0$.

A similar procedure can be used for the limit $\kappa_2 \to 0$, though in this case the breakdown of the Helmholtz decomposition mentioned after (3.9) introduces additional complications, and we do not reproduce the details here. Another example of a problem involving an infinite linear system of equations in which certain coefficients are singular, but where a nontrivial solution still exists, can be found in [30].

References

[1] F. Ursell. Surface waves on deep water in the presence of a submerged circular cylinder I. *Proc. Camb. Phil. Soc.*, 46:141–152, 1950.

[2] F. Ursell. Surface waves on deep water in the presence of a submerged circular cylinder II. *Proc. Camb. Phil. Soc.*, 46:153–158, 1950.

[3] W. E. Bolton and F. Ursell. The wave force on an infinitely long circular cylinder in an oblique sea. *J. Fluid Mech.*, 57:241–256, 1973.

[4] R. D. Gregory. An expansion theorem applicable to problems of wave propagation in an elastic half-space containing a cavity. *Proc. Camb. Phil. Soc.*, 63:1341–1367, 1967.

[5] R. D. Gregory. The propagation of waves in an elastic half-space containing a cylindrical cavity. *Proc. Camb. Phil. Soc.*, 67:689–710, 1970.

[6] V. W. Lee and M. D. Trifunac. Response of tunnels to incident SH-waves. *Journal of the Engineering Mechanics Division (ASCE)*, 105(4):643–659, 1979.

[7] Michael E. Manoogian and Vincent W. Lee. Diffraction of SH-waves by subsurface inclusions of arbitrary shape. *J. Engrg. Mech.*, 122(2):123–129, 1996.

[8] C. Smerzini, J. Avilés, R. Paolucci, and F. J. Sánchez-Sesma. Effect of underground cavities on surface earthquake ground motion under SH wave propagation. *Earthquake Engineering and Structural Dynamics*, 38:1441–1460, 2009.

[9] F. Höllinger and F. Ziegler. Scattering of pulsed Rayleigh surface waves by a cylindrical cavity. *Wave Motion*, 1:225–238, 1979.

[10] V. W. Lee and J. Karl. Diffraction of SV waves by underground, circular, cylindrical cavities. *Soil Dynamics and Earthquake Engineering*, 11:445–456, 1992.

[11] S. K. Datta and N. El-Akily. Diffraction of elastic waves by cylindrical cavity in a half-space. *J. Acoust. Soc. Am.*, 64(6):1692–1699, 1978. Erratum: 65(5):p.1342, 1979.

[12] N. El-Akily and S. K. Datta. Response of a circular cylindrical shell to disturbances in a half-space. *Earthquake Engineering and Structural Dynamics*, 8:469–477, 1980.

[13] N. El-Akily and S. K. Datta. Response of a circular cylindrical shell to disturbances in a half-space—numerical results. *Earthquake Engineering and Structural Dynamics*, 9:477–487, 1981.

[14] C. C. Mei. Extensions of some identities in elastodynamics with rigid inclusions. *J. Acoust. Soc. Am.*, 64(5):1514–1522, 1978.

[15] J. N. Newman. Interaction of waves with two-dimensional obstacles: a relation between the radiation and scattering problems. *J. Fluid Mech.*, 71:273–282, 1975.

[16] Fred L. Neerhoff. Reciprocity and power-flow theorems for the scattering of plane elastic waves in a half space. *Wave Motion*, 2(2):99–113, 1980.

[17] F. C. P. de Barros and J. E. Luco. Diffraction of obliquely incident waves by a cylindrical cavity embedded in a layered viscoelastic half-space. *Soil Dynamics and Earthquake Engineering*, 12(3):159–171, 1993.

[18] W. I. Liao, C. S. Yeh, and T. J. Teng. Scattering of elastic waves by a buried tunnel under obliquely incident waves using t matrix. *Chinese Journal of Mechanics, A*, 24(4):405–418, 2008.

[19] F. Ursell. Trapping modes in the theory of surface waves. *Proc. Camb. Phil. Soc.*, 47:347–358, 1951.

[20] P. McIver and D. V. Evans. The trapping of surface waves above a submerged horizontal cylinder. *J. Fluid Mech.*, 151:243–255, 1985.

[21] M. A. Biot. Propagation of elastic waves in a cylindrical bore containing a fluid. *J. Appl. Phys.*, 23(9):997–1005, 1952.

[22] A. Boström and A. Burden. Propagation of elastic surface waves along a cylindrical cavity and their excitation by a point force. *J. Acoust. Soc. Am.*, 72(3):998–1004, 1982.

[23] K. F. Graff. *Wave Motion in Elastic Solids*. Oxford University Press, 1975.

[24] G. N. Watson. *A Treatise on the Theory of Bessel Functions*. Cambridge University Press, 2nd edition, 1944.

[25] A. M. Turing. A method for the calculation of the zeta-function. *Proceedings of the London Mathematical Society*, 48(3):180–197, 1945.

[26] H. Fossen. *Structural Geology*. Cambridge University Press, 2010.

[27] C. M. Linton and D. V. Evans. The radiation and scattering of surface waves by a vertical circular cylinder in a channel. *Phil. Trans. R. Soc. Lond., A*, 338:325–357, 1992.

[28] Norman Bleistein and Richard A. Handelsman. *Asymptotic Expansions of Integrals*. Dover Publications, New York, 1986. Originally published in 1975.

[29] F. W. J. Olver, D. W. Lozier, R. F. Boisvert, and C. W. Clark, editors. *NIST Handbook of Mathematical Functions*. NIST and Cambridge University Press, 2010.

[30] C. M. Linton and I. Thompson. Resonant effects in scattering by periodic arrays. *Wave Motion*, 44:167–175, 2007.